A Modeling Study in the Regulation of Stress on Neuronal Plasticity

by

PENGCHENG XIAO

Presented to the Faculty of the Graduate School of

The University of Texas at Arlington in Partial Fulfillment

of the Requirements

for the Degree of

DOCTOR OF PHILOSOPHY

THE UNIVERSITY OF TEXAS AT ARLINGTON

August 2015

To God

Who create all the beauties.

To my mother Yuxiang Wang and my father Zhihe Xiao

who set the example and who made me who I am.

To my wife Niuniu Xiao

you make me the Happiest man in the world!

ACKNOWLEDGEMENTS

I would like to thank my supervising professor Dr. Jianzhong Su for constantly motivating and encouraging me, and also for his invaluable advice during the course of my doctoral program. I wish to thank my committee members Dr. Tuncay Aktosun, Dr. Benito Chen-Charpentier, Dr. Hristo V. Kojouharov, Dr. Ren-Cang Li, and Dr. Guojun Liao for their interest in my research and for taking time to serve in my dissertation committee.

I would also like to extend my appreciation to the Department of Mathematics at The University of Texas at Arlington for providing financial support in my doctoral program. I am grateful to all the teachers who taught me during my academic career, first in China, then in the Unites States. I would like to thank Dr. Zhaosheng Feng and Dr. Xiaohui Wang for encouraging and inspiring me to pursue graduate studies.

Finally, I would like to express my deep gratitude to my parents Zhihe Xiao and Yuxiang Wang, who have encouraged and inspired me and sponsored my undergraduate and graduate studies. I am extremely fortunate to be so blessed. I am also extremely grateful to my wife Niuniu for her sacrifice, encouragement and patience. I thank God for all the blessing in my life.

July 24, 2015

ABSTRACT

A Modeling Study in the Regulation of Stress on Neuronal Plasticity

Pengcheng Xiao, Ph.D.

The University of Texas at Arlington, 2015

Supervising Professor: Jianzhong Su

How stress can affect human cognitive functions has been a very popular topic for researchers from different fields including physiology, psychology, biology, neuroscience, and applied mathematics. Hypothalamic−pituitary−adrenal (HPA) axis plays an important role in response to stress by releasing hormones, and level of glucocorticoid has been widely considered to be one key factor to distinguish people with different stress disorder. Emerging evidence has shown that glucocorticoid act on glutamate neurotransmission system and consequently influences neuronal activities's cognitive function. It changes in the glutamate release and induces synapse plasticity change. Spike-Timing Dependent Plasticity (STDP) is one of the important neuroscience foundations for cognitive function. In this dissertation, we incorporate the HPA axis and CA1 neuron models to explore the plasticity outcome based on different type of stress. Various of spikes will be applied to test the Spike-Timing Dependent Plasticity in different durations. The results in different facets show that CA1 neuron potentiation changes due to different stress input.

TABLE OF CONTENTS

LIST OF ILLUSTRATIONS

LIST OF TABLES

CHAPTER 1

INTRODUCTION

In this dissertation, a unified mathematical model of stress disorder and neuronal plasticity theory will be presented. The goal of this research is to explore the resulting synaptic plasticity variations between healthy people and people with post-traumatic stress disorder (PTSD).

In the first part of the dissertation we are interested in hypothalamic -pituitary-adrenal (HPA) axis actions. The HPA axis is a major part of the neuroendocrine system that controls reactions to stress. Experimentally, the alternation of cortisol, a hormone secreted in the adrenal cortex, is widely considered to be the informative-biomarker that distinguishes people with anxiety disorders from healthy people.

The second part of this research is spike timing−dependent plasticity (STDP) under stress condition. It is widely accepted that synaptic plasticity is underpinning learning and memory functions in the brain. The STDP protocol that involves triggering synaptic inputs with postsynaptic spikes with a relative timing is used to induce persistent changes in the strength of synaptic connection between neurons. The resulting plasticity depends on the timing difference of spike inputs in different parts. In this dissertation, we take advantage of some latest research in developing several ideas of describing plasticity.

Research suggests that the stress−induced release of cortisol prompts changes in glutamate neurotransmission, thereby influencing some aspects of cognitive processing. This relation connects the two sets of equations used in the modeling. To the

best of our knowledge, this is the first computational model for describing synaptic plasticity for human with PTSD.

This dissertation is organized as follows. Chapter 2: "Background", we describe the hypothalamic−pituitary−adrenal (HPA) axis, post-traumatic stress disorder (PTSD), and spike timing−dependent plasticity (STDP) and their importance. In Chapter 3: "Modeling", we present a HPA axis model, a subsystem of our model and also the bifurcation analysis for this model. Then we describe a two compartments CA1 neuron model. Finally we discuss how we couple the two models to our model. In Chapter 4: "Numerical Simulation", we present the methods that are used to measure the resulting synaptic plasticity for human with PTSD and normal people, and also we present the resulting synaptic plasticity with acute stress imposed in our model. In Chapter 5: "Conclusion and future work", we summarize the major findings from our research and also discuss our future research plan.

CHAPTER 2

BACKGROUND

2.1 Hypothalamic-Pituitary-Adrenal (HPA) Axis

The anatomical structure that mediate the stress response is mainly in the central nervous system (CNS) and its peripheral organs. The principal effectors of the stress response are localized in the paraventricular nucleus of the hypothalamus, the anterior lobe of the pituitary gland, and the adrenal gland. This collection of brain areas is commonly referred to as the Hypothalamic-Pituitary-Adrenal (HPA) axis [1].

The HPA axis plays an important role in balancing hormonal levels for brain, and generate high concentration of hormones in response to stress, which leads to downstream changes [2]. To response stress over a period of time, the paraventricular nucleus of hypothalamus that contains neuroendocrine neurons releases corticotropin-releasing hormone (CRH). The anterior lobe of the pituitary gland is stimulated by CRH to secrete adrenal corticotrophic hormone (ACTH). The adrenal cortex then produces cortisol hormones in response to stimulation by ACTH. Cortisol is a major stress related hormone and has effects on many tissues in the body, particularly in the brain. In the brain, cortisol acts on two types of receptors: mineralocorticoid receptors and glucocorticoid receptors [3, 4, 5]. For down regulating CRH, it is known that cortisol inhibits the secretion of CRH through glucocoticoid receptors complex [6]. With a strong affinity to glucocoticoid receptors complex, cortisol in turn acts on the hypothalamus and pituitary in a negative feedback cycle to down regulate the production of cortisol [7].

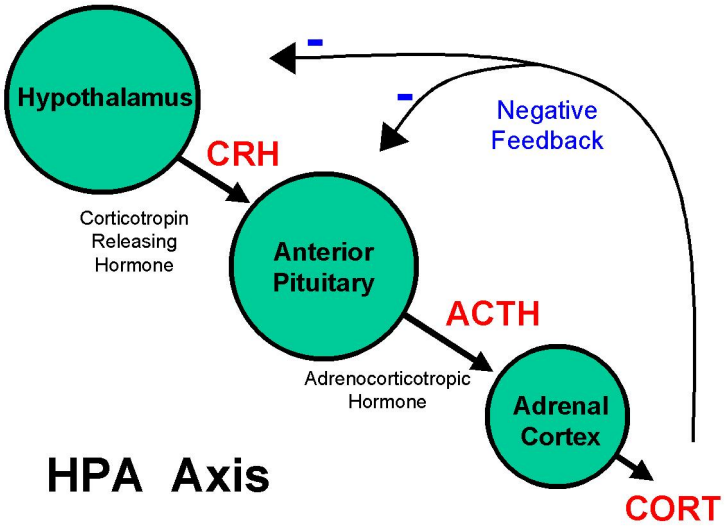

Figure 2.1. A diagram for Hypothalamic-Pituitary-Adrenal (HPA) axis. In response to stress, the hypothalamus releases CRH, which activates the pituitary and secrete of ACTH. ACTH stimulates adrenal to secrete glucocorticoid. Glucocorticoid performs a negative feedback on the secretion of CRH and ACTH.

2.1.1 Glucocorticoids on Stress

Modulation of stress reactions is an important function for glucocorticoids. Previous studies [8] show that the type of stressor is one main factor that affects the different activations ways for HPA axis during chronic stress [8]. Stressors type can be uncontrollable, threaten physical integrity, or involve trauma tend to have a high, flat diurnal profile of cortisol release (with lower than normal levels in the morning and higher than normal levels in the evening) resulting in a high overall of daily cortisol release. However, short term stressors tend to produce higher than normal morning cortisol. Stress hormone release tends to decline gradually after a stressor occurs[8]. For people with post-traumatic stress disorder (PTSD), researchers found that there appears to be lower than normal cortisol release, and it is thought that a blunted hormonal response to stress may predispose a person to develop PTSD [9, 10, 11].

2.1.2 Glucocorticoids on cognitive function

It is believed that glucocorticoids, along with adrenaline, act on hippocampus to enhance the formation of flashbulb of events associated with strong emotions, both positive and negative [12]. A large number of studies have confirmed this hypothesis, whereby blocks of either glucocorticoids or noradrenaline activity impaired the recall of emotionally relevant information [13, 14]. The effect that glucocorticoids have on memory may be due to abnormality of the CA1 area of the hippocampal formation. In multiple animal studies, prolonged stress have shown the change of the neurons in this area of the brain, which has been connected to the memory performance [15, 16].

Studies have shown circulating levels of glucocorticoids verses memory performance follow an upside down U pattern as in Figure 2.2 [17]. Long term potentiation (LTP) is optimal when glucocorticoids levels are mildly elevated, whereas significant decreases of LTP are observed after adrenadectomy (low glucocorticoids level) or after exogenous glucocorticoids administration (high glucocorticoids level) [17]. Elevated levels of glucocorticoids enhance memory for emotionally arousing events, but trauma events lead more often than not to poor memory [17], as tested in experiments that emulate classroom learning.

2.2 Post-traumatic Stress Disorder (PTSD)

Post-traumatic stress disorder (PTSD) may develop after a person is exposed to one or more traumatic events, such as major stress, sexual assault, terrorism, or other threats on a person's life [18]. The diagnosis may be given when a group of symptoms, such as disturbing recurring flashbacks, avoidance or numbing of memories of the event, and hyperarousal, continue for more than one month after the occurrence of a traumatic event [18].

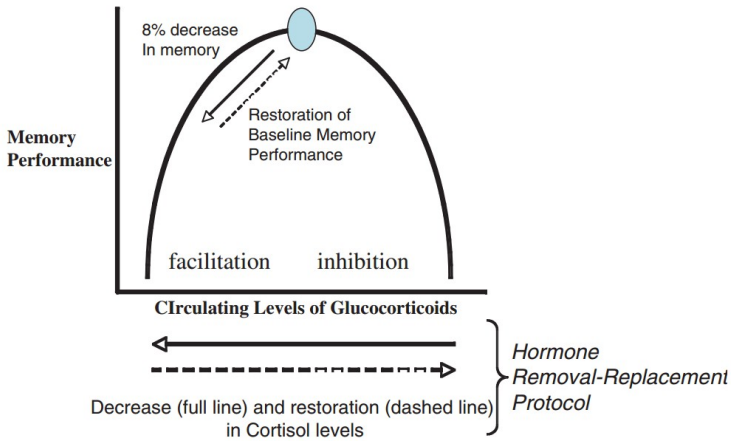

Figure 2.2. A Schematic Hormone in representation of the modulation of the memory performance by Lupien et al (2007). After cortisol decrease, a 8% decrease in declarative memory performance that was restored to placebo level after restoration of circulating levels of cortisol by pharmacological infusion of hydrocortisone.

Most people having experienced a traumatizing event will not develop PTSD [19]. People who experience assault based trauma are more likely to develop PTSD, as opposed to people who experience non-assault based trauma such as witnessing trauma, accidents, and fire events [20]. Children are less likely to experience PTSD after trauma than adults, especially if they are under ten years of age [19]. War veterans are commonly at risk of PTSD. The characteristic symptoms are considered acute if lasting less than three months, and chronic if lasting three months or more, and with delayed onsets if the symptoms first occur after six months or some years later [18]. PTSD is distinct from the briefer acute stress disorder, and can cause clinical impairment in significant areas of functions [21, 22, 23].

2.2.1 PTSD and Glucocorticoids Dynamics

Compared to the cortisol level in normal human subjects, significantly lower cortisol concentration was observed in PTSD subjects over a 24 hours period [9]. As it is well known that HPA axis is responsible for coordinating the hormone response

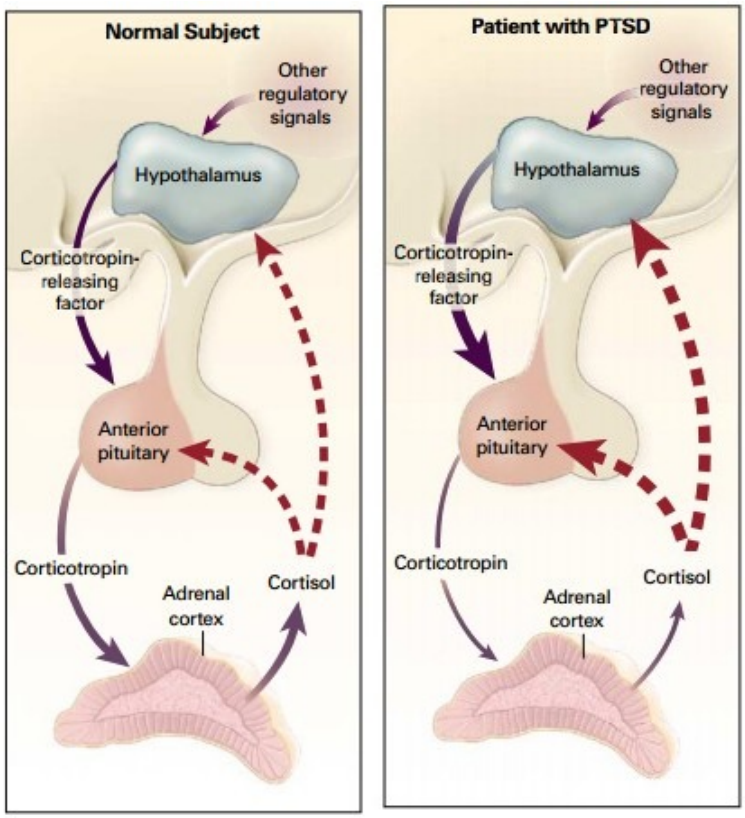

Figure 2.3. Responses to stress in a Normal Subject and a Patient with PTSD by Yehuda(2002). In patients with PTSD, levels of cortisol are low and levels of corticotropin-releasing factor are high. In addition, the sensitivity of the negative-feedback system of the hypothalamicpituitaryadrenal axis is increased in patients with PTSD.

to stress, Yehuda [24] first proposed the hypothesis that the lower cortisol level is due to strong negative feedback inhibition of cortisol in HPA axis (Figure 2.3). In a more recent work [10], cortisol patterns collected from PTSD subjects and normal subjects are evaluated to support the hypothesis. Although many results are published on research experiments, the consequence of cortisol alternation is still considered as an unsolved problem for the research of PTSD. In this dissertation, we treat cortisol level is one main dependent variable for modelling the relationship between PTSD and neuron plasticity.

2.3 Synaptic Plasticity

Synaptic plasticity is the ability of synapses to change the strengths (stronger or weaker) over time in response to neuronal activities [25]. Researchers have found that synaptic plasticity in both excitatory and inhibitory synapses is highly related to the release of calcium [26]. Two main underlying mechanisms that cooperate to achieve synaptic plasticity are proposed: (i) the change of quantity of neurotransmitters released into a synapse, and (ii) the change of efficiency that neurons receptors responding to those neurotransmitters due to calcium change [26, 27]. Since the two important cognitive functions, memory and learning, are postulated by dynamically alternating coupling strengths of neurons in the brain. Understanding the cellular mechanisms underlying such functional plasticity has been a long standing challenge in neuroscience [28]. In this dissertation, we assume the postsynaptic calcium concentration as the key biomarker for synaptic plasticity change.

2.3.1 Long-term Potentiation (LTP) and Depression (LTD)

In neuroscience, long-term potentiation (LTP) and long term-depression (LTD) are two main phenomena that reflects synaptic plasticity.

Long-term potentiation is a persistent process that strengths the synapse with the recent patterns of activity. Although the discovery of LTP was over 40 years ago, its molecular mechanism was not fully understood until recently [29]. In the middle of 1980s, researchers discovered that antagonises of NMDA type of glutamate receptor prevents LTP, but there is no effect on the synaptic response evoked by low-frequency stimulation of the Schaffer collaterals [29]. In *Neuroscience, 4ed*, Purves D *et al* state the molecular underpinning of LTP:

"The NMDA receptor is permeable to Ca^{2+}, but is blocked by physiological concentrations of Mg^{2+}. This property provides a critical insight into how LTP is

selectively induced by high-frequency activity. During low-frequency synaptic transmission, glutamate released by the Schaffer collaterals binds to both NMDA-type and AMPA/kainate-type glutamate receptors. While both types of receptors bind glutamate, if the postsynaptic neuron is at its normal resting membrane potential, the pore of the NMDA receptor channel will be blocked by Mg^{2+} ions and no current will flow. Under such conditions, the EPSP will be mediated entirely by AMPA receptors. Because blockade of the NMDA receptor by Mg^{2+} is voltage-dependent, the function of the synapse changes markedly when the postsynaptic cell is depolarized. Thus, high-frequency stimulation will cause summation of EPSPs, leading to a prolonged depolarization that expels Mg^{2+} from the NMDA channel pore. Removal of Mg^{2+} allows Ca^{2+} to enter the postsynaptic neuron and the resulting increase in Ca^{2+} concentration with the dendritic spines of the postsynaptic cell turns out to be trigger for LTP. The NMDA receptor thus behaves like a molecular coincidence detector. Several sorts of observations have confirmed that a rise in the concentration of Ca^{2+} in the postsynaptic CA1 neuron, due to Ca^{2+} ions entering through NMDA receptors, serves as a second messenger signal that induces LTP. ”

If synapses were only strengthened as a result of LTP, eventually they would reach some maximum level to make it difficult to encode information [29]. To prevent neurons from becoming static, other processes must selectively weaken specific set of synapses [29]. LTD is such a process. In early 1980s, Bienenstock, Cooper and Munro proposed that a certain threshold exists such that a level of postsynaptic response below the threshold will lead to LTD while above it will lead to LTP, and further they proposed that the level of this threshold is not fixed, it depends on the average amount of postsynaptic activity [30].

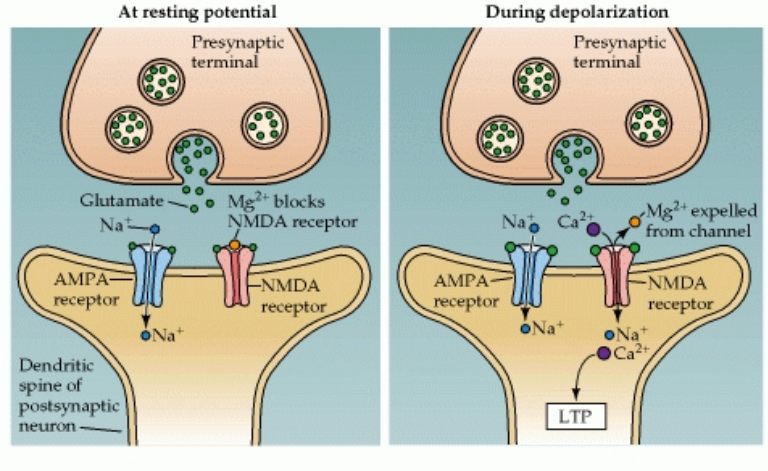

Figure 2.4. The NMDA receptor channel can open only during depolarization of the postsynaptic neuron from its normal resting level. Depolarization expels Mg^{2+} from the NMDA channel, allowing current to flow into the postsynaptic cell. This leads to Ca^{2+} entry, which in turn triggers LTP. (Neuroscience 4ed, Purves D. PP. 191 After Nicoll, Malenka and Kauer, 1988.).

2.3.2 Spike Timing-Dependent Plasticity (STDP)

In 1949, Hebb [35] proposed that the strength of synapse should increase under the condition that presynaptic cells are taking part in the postsynaptic cells' firing effectively. Hebb's postulate has a huge influence for many subsequent experimental research. In the late 1990s, researchers [31, 32, 33, 34] made a great leap forward in decrypting the governing rule for synaptic plasticity. They found that the temporal order of pre- and postsynaptic spiking determines the synapse plasticity output, meaning LTP or LTD. Because of the order and timing dependence, this phenomenon was termed spike timing-dependent plasticity (STDP) [36]. When presynaptic spiking precedes postsynaptic spiking (hereafter referred to as pre-post) within a window of tens of milliseconds, synapses potentiate, whereas a spiking sequence of reversed order (post-pre) leads to the depress of synapses. While the dependence of synaptic

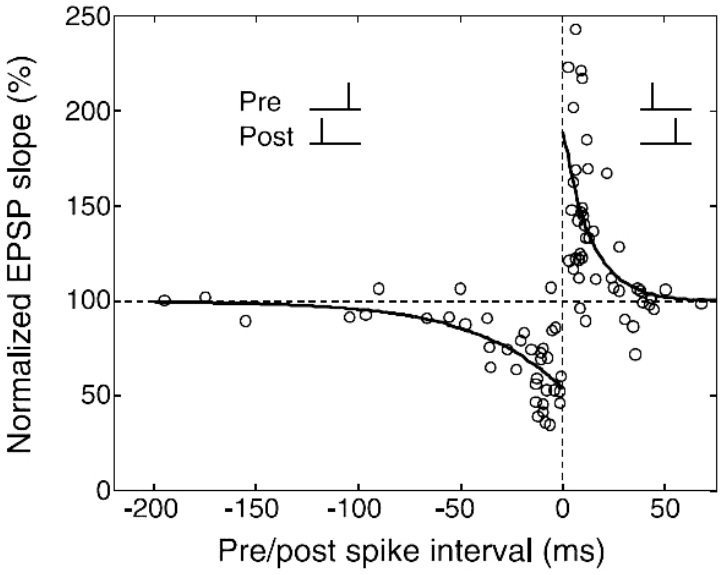

Figure 2.5. Illustration of spike timing dependent plasticity time windows, taken from Bi and Poo (1998). The STDP function shows the change of synaptic connections as a function of the relative timing of pre- and postsynaptic spikes.

modification on the pre/post spike order is commonly observed, the width of the STDP window varies [37].

2.4 Importance of Building Models

In this dissertation, we are interested in modeling the relationship between different stress input and corresponding synaptic plasticity output. The key point for this research is to understand the mechanisms for, in this case the alternations of glucocorticoid hormone associated with different stress inputs, that give rise to changes in synaptic strength observed during the Spike Timing Dependent Plasticity protocol.

Insights gained into the relationship between stress and cognitive function by studying Spike Timing Dependent Plasticity will lead a better understanding of plasticity under broader circumstances. With neuronal plasticity mechanisms operating

under different stress conditions, it will also be possible to predict how stress related hormone such as glucocoticoid affect neuron plasticity, and subsequently affect human cognitive function. Also, the model provides for the time history of the neuron plasticity under various spike input patterns, this will be valuable for understanding the complexity of this dynamical system.

CHAPTER 3

MODELING

3.1 HPA axis model

3.1.1 General Description

In Chapter 2, section 2.1. We already have introduced the mechanism of HPA axis that responses to stress, and mainly three hormones are involved for the interactions. The return to base hormone levels over time is a key feature for the system when it is in a normal status [38].

In previous HPA axis modelling, many researchers treat the dynamical system as three parts interactions, including hypothalamus, pituitary, and adrenal. More details can be seen from F. Vinther *et al* 's summary [38]. Corticotropin-releasing hormone (CRH) is released at hypothalamus with the stress stimulations. CRH goes through blood to pituitary and stimulates the release of adrenal corticotrophic hormone (ACTH). ACTH reaches to adrenal gland to stimulate the cortisol secretion. To maintain the regular dynamics, cortisol in turn performs a negative feedback on hypothalamus and pituitary to regulate the secretion of CRH and ACTH. The model presented by Gupta *et al* [39] consists four parts including GR homodimerizes to reveal bistability of HPA axis. Followed this idea, we use the similar proof process with F.Vinther [38] and construct an theoretical HPA axis model including GR complex, we term our model Extended Minimal Model (EMM) and details for model constructing and characteristic proof are in Appendix A.

From the model simulation view, we want to use a model that can have as many HPA axis properties like negative feedback, circadian and ultradian rhythms

of hormone concentrations et as it can. In 2012, Sriram *et al* [7] presented a model that can exhibit both circadian and ultradian oscillations and fit the data for PTSD subjects and people with long time depression from Yehuda *et al* [10, 24] . In this dissertation, we will make full use of this model to compute the synaptic plasticity for people with PTSD.

To develop this model, Sriram *et al* [7] made two assumptions: (i) Apart from dilution/autonomous degradation, Michaelis-Menten kinetics are separately considered for degradation of the hormones and hormone complexes within each specific region of the brain; and (ii) a sufficient number of molecules is present for reactions so that stochastic fluctuations are eliminated [7].

We present below the cortisol dynamics model based on four variable differential equations here. CRH stands for concentration of corticotrophin-releasing hormone, $ACTH$ stands for adrenal-corticotrophin hormone, $CORT$ for cortisol, G for glucocorticoid receptor and GR for glucocorticoid receptor complex. Then,

$$\frac{d[CRH]}{dt} = k_{stress}\frac{K_i^{n2}}{K_i^{n2} + [GR]^{n2}} - V_{S3}\frac{[CRH]}{k_{m1} + [CRH]} - K_{d1}[CRH] \tag{3.1}$$

$$\frac{d[ACTH]}{dt} = K_{P2}\frac{K_i^{n2}}{K_i^{n2} + [GR]^{n2}} - V_{S4}\frac{[ACTH]}{K_{m2} + [ACTH]} - K_{d2}[ACTH] \tag{3.2}$$

$$\frac{d[CORT]}{dt} = K_{P3}[ACTH] - V_{S5}\frac{[CORT]}{K_{m3} + [CORT]} - K_{d3}[CORT] \tag{3.3}$$

$$\frac{d[GR]}{dt} = K_b[CORT]([G_{tot}] - [GR]) + V_{S2}\frac{[GR]^{n1}}{K1^{n1} + [GR]^{n1}} - K_{d5}[GR] \tag{3.4}$$

where $G_{tot} = G + GR$ is the total glucocorticoid receptor. Among the key parameters, K_{stress} represents the level of stress, K_i is the inhibition constant that

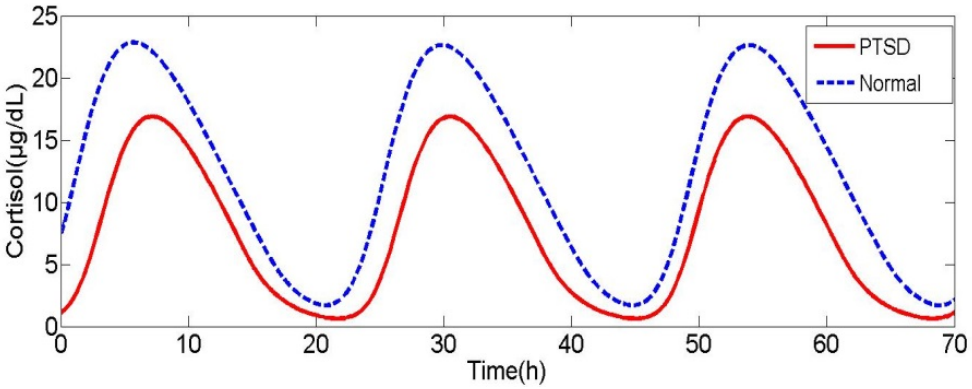

Figure 3.1. The comparison of Cortisol levels in time course in Normal state and in PTSD state during a 70-hour period, Cortisol unit is μg/dL. The data are simulated from the mathematical model. Both patterns are periodic with period being 24 hour.

regulates the strength of the negative feedback loop, an important biophysical parameter responsible for PTSD when the feedback loop is overly strong. The parameters $V_{sj}, j = 3, 4, 5$ are rate constants for hormones CRH, $ACTH$, and $CORT$ degradations through saturation kinetics. The parameters $K_{mj}, j = 1, 2, 3$ are Michaelis-Menton constants, $K_{dj}, j = 1, 2, 3, 5$ are autonomous degradation constants, $K_{pj}, j = 2, 3, 4$ are production rates of $ACTH$, $CORT$, and GR, $n1$, $n2$ are Hill constants and $K1$ is an activation constant.

3.1.2 Simulation and Bifurcation Analysis

Based on Equations (3.1 - 3.4), we calculate the normal and PTSD states Cortisol dynamics time course with initial values from their (unstable) equilibrium points. Both normal and PTSD time courses converge quickly to 24-hour periodic patterns in Figure 3.1, representing human hormonal cycles. To see the difference in the normal and PTSD states, we calculate bifurcation diagrams, and the two parameters Hopf bifurcation diagrams with stress versus CRH degradation rate in Figure 3.2 and Figure 3.3, and stress versus ACTH degradation in Figure 3.4 and Figure 3.5 show

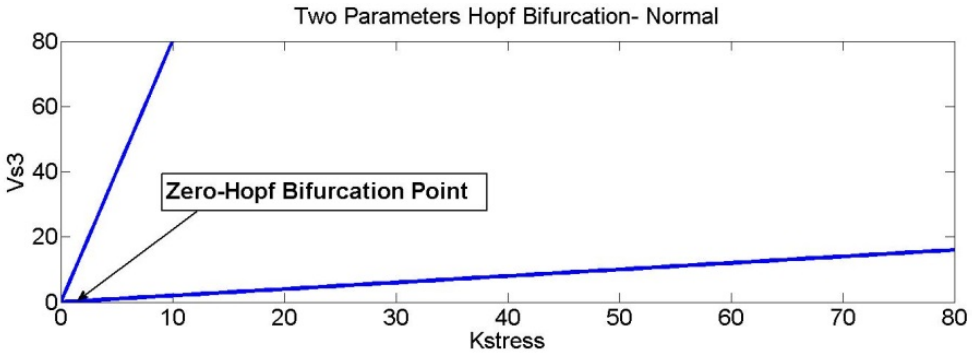

Figure 3.2. The Hopf bifurcation diagram of the system in normal conditions. Only one Zero-Hopf Bifurcation occurs in lower k_{stress} and V_{s3} values.

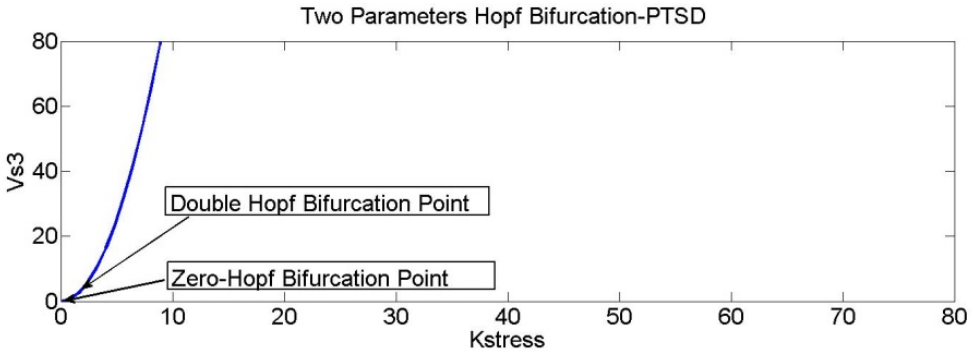

Figure 3.3. The Hopf bifurcation diagram of the system in PTSD patients. One Zero-Hopf Bifurcation occurs very fast, and then another Double-Hopf Bifurcation point comes out for k_{stress} and V_{s3} bifurcation. Both of them were found in lower k_{stress} and V_{s3} values.

distinct cortisol dynamics in normal and PTSD states. All the two parameters bifurcation analysis are calculated in software toolbox MATCONT [40] and XPPAUT [41].

Definition 1. ***The Zero-Hopf bifurcation*** *is a bifurcation of an equilibrium point in a two-parameter family of autonomous ODEs at which the critical equilibrium has a zero eigenvalue and a pair of purely imaginary eigenvalues [42].*

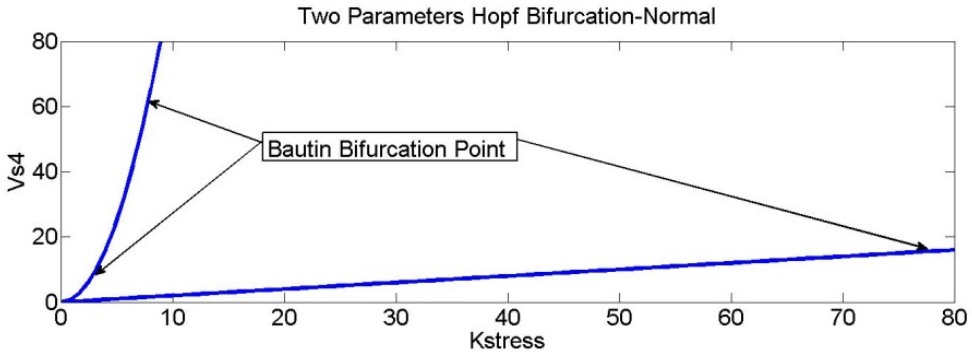

Figure 3.4. The Hopf bifurcation diagram of the system in normal conditions. Two bautin bifurcation points were found in a lower k_{stress} value with different V_{s4} values , and another bautin bifurcation point terminated at a hight k_{stress} value and lower V_{s4}.

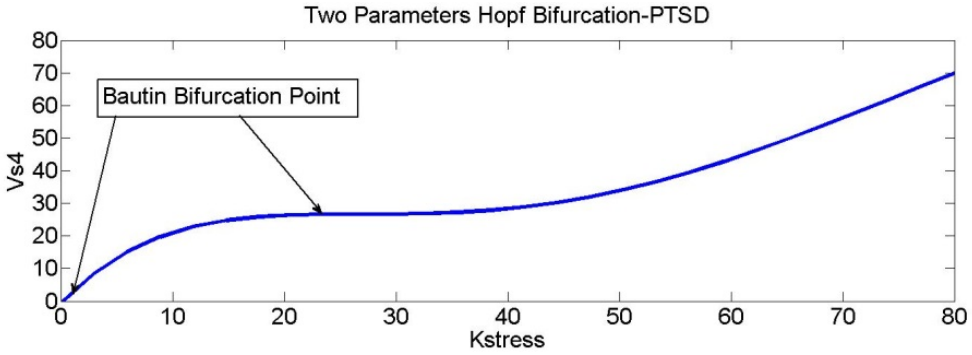

Figure 3.5. The Hopf bifurcation diagram of the system in PTSD patients. One bautin bifurcation point was found in lower k_{stress} and V_{s4} values, and another bautin bifurcation point terminated at medium k_{stress} and V_{s4} values.

Definition 2. ***Double Hopf bifurcation*** *is a bifurcation of an equilibrium point in a two-parameter family of autonomous ODEs at which the critical equilibrium has two pairs of purely imaginary eigenvalues that go through imaginary axis [42].*

Definition 3. ***The Bautin bifurcation*** *is a bifurcation of an equilibrium in a two-parameter family of autonomous ODEs at which the critical equilibrium has a pair of purely imaginary eigenvalues and the first Lyapunov coefficient for the Andronov-Hopf bifurcation vanishes [42].*

In Figure 3.2, we see that for normal state, the stress indicator K_{stress} and V_{s3} will generate one Zero-Hopf bifurcation point when both of the values are very small. This bifurcation may lead to a local birth of chaos [42]. However, in Figure 3.3, the PTSD state has one Zero-Hopf bifurcation as compared to the normal state in Figure 3.2, then another Double Hopf bifurcation happens when K_{stress} and V_{s3} become bigger. The Double Hopf bifurcation can also imply periodicity [42]. This might reveal the fact that the negative feedback function for CRH in cortisol dynamic for human in PTSD state is more complicated than that of normal state.

Figure 3.4 and 3.5 depict the two parameters Hopf bifurcations in the normal state and the PTSD state. Three Bautin bifurcation occurs in the normal state. Two of them generated for small value of K_{stress} with V_{s4} varying from 10 to 70, the last one occurs in a large value of K_{stress} and when V_{s4} is close to 20. For PTSD state, one Bautin bifurcation point occurs when the values of K_{stress} and V_{s4} are small. Another Bautin bifurcation occurs when K_{stress} with V_{s4} are between 20 and 30. Since the negative feedback function for $ACTH$ for PTSD state is strengthened as compared to that in normal state, this can explain the number of Bautin bifurcation points for PTSD state is less than that of normal state.

3.1.3 Acute Stress for Normal and PTSD subjects

We explore the cortisol dynamics under the situation that an acute stress occurs between normal subject and PTSD subject. In mathematics view, we will cooperate the stress parameter k_{stress} with a pulse function $f(t)$. The pulse function represents a short step pulse that is turned on to initiate the acute stress and then turned off after a reasonable time duration (2 hours - 4 hours). More details can be seen in Chapter 4.

3.2 CA1 Neuron Model

3.2.1 Build the model

We now follow Rubin et al [43] in testing the effect of PTSD in a two-compartment hippocampus CA1 model consisting of a soma and a localized dendritic region. The model allows for consideration of back-propagation of action potentials initiated experimentally in the soma. Their model was a calibrated two-compartment CA1 pyramidal cell model, reduced from an earlier multi-compartment model of Poirazi et al [44]. Two compartments consist of a soma compartment and a dendritic compartment (spine) matching a single dendritic region. The voltage potentials for both compartments are

$$\frac{dv}{dt} = (I_L + I_{Na} + I_K + I_{Ca} + I_{coup} + I_{in})/C_m \tag{3.5}$$

where I_L is the leak current, I_{Na} is the sodium current, I_K is the sum of potassium currents, I_{Ca} is the calcium current, I_{coup} is the electrical coupling between the compartments, I_{in} is the soma current and C_m is the normalized the membrane capacitance. Calcium currents, whose behaviour measure plasticity, satisfy

$$\chi'_{soma} = \Phi I_{Ca,soma} - \beta_{soma}(\chi_{soma} - \chi_{0,soma}) + (\chi_{spine} - \chi_{soma})/d - (\beta_{soma}/\eta_{buff})\chi_{soma}{}^2 \tag{3.6}$$

$$\chi'_{spine} = \Phi(I_{Ca,spine}+I_{Ca,NMDA}) - \beta_{spine}(\chi_{spine}-\chi_{0,spine}) - (\beta_{spine}/\eta_{buff})\chi_{spine}{}^2 - \beta_{buff}\chi_{spine} \tag{3.7}$$

where χ_{soma}, χ_{spine} are calcium concentrations in soma and spine respectively, and $\chi_{0,soma}$, $\chi_{0,spine}$ are their resting calcium levels, d is the calcium diffusion rate from soma to spine, η_{buff} is the strength of nonlinear calcium buffering, β_{soma} and β_{buff}

are buffering constants, $I_{ca,spine}$ and $I_{ca,soma}$ denote voltage-gated calcium currents and M is a unit conversion constant.

$$I_{Ca,NMDA} = -G_{Ca,NMDA} S_{NMDA} M_{Ca,NMDA}(v_{spine} - v_{Ca,rev}). \tag{3.8}$$

The total electric current through $NMDA$ channel is

$$I_{syn,NMDA} = -G_{syn,NMDA} S_{NMDA} M_{syn,NMDA}(v_{spine} - v_{syn,rev}) \tag{3.9}$$

where $G_{syn,NMDA}$ is the channel conductance, S_{NMDA} represents the activation of $NMDA$ channel, $M_{syn,NMDA}$ measures the removal of magnesium block of the appropriate ionic flow and $v_{syn,rev}$ is the reversal potential of calcium current.

$$M_{syn,NMDA} = 1.0/[1.0 + 0.3(Mg)exp(-0.062 v_{spine})]. \tag{3.10}$$

AMPA synatpic currents are similar as follows:

$$I_{syn,AMPA} = -G_{AMPA} S_{AMPA}(v_{spine} - vsyn, rev). \tag{3.11}$$

The activation equations [45, 46] of NMDA and AMPA currents are

$$S_x = S_{x,fast} + S_{x,slow} + S_{x,rise}, \tag{3.12}$$

where x is $NMDA$ or $AMPA$,

$$S'_{NMDA,rise} = -\Phi(1 - S_{NMDA,fast} - S_{NMDA,slow}) f_{pre}(t) - S_{NMDA,rise}/\tau_{NMDA,rise}, \tag{3.13}$$

$$S'_{NMDA,fast} = \Phi(0.527 - S_{NMDA,fast}) f_{pre}(t) - S_{NMDA,fast}/\tau_{NMDA,fast}, \tag{3.14}$$

$$S'_{NMDA,slow} = \Phi(0.473 - S_{NMDA,slow}) f_{pre}(t) - S_{NMDA,slow}/\tau_{NMDA,slow}, \quad (3.15)$$

$$S'_{AMPA,rise} = -\Phi(1 - S_{AMPA,fast} - S_{AMPA,slow}) f_{pre}(t) - S_{AMPA,rise}/\tau_{AMPA,rise}, \quad (3.16)$$

$$S'_{AMPA,fast} = \Phi(0.903 - S_{AMPA,fast}) f_{pre}(t) - S_{AMPA,fast}/\tau_{AMPA,fast}, \quad (3.17)$$

$$S'_{AMPA,slow} = \Phi(0.097 - S_{AMPA,slow}) f_{pre}(t) - S_{AMPA,slow}/\tau_{AMPA,slow}, \quad (3.18)$$

$f_{pre}(t)$ stands for a step pulse that is turned on to initiate the postsynaptic effect when a presynaptic spike occurs [43].

3.2.2 Pre and Post-synaptic Spike

In the two compartments CA1 neuron model, the postsynaptic spike is stimulated in soma, while the presynaptic spike acts on spine's receptors. So the calcium influx in the spine will be considered the biomarker for change of synapse plasticity.

Here we briefly show the single presynaptic spike at t=11ms in Figure 3.6 and postsynaptic spike at t=11ms in Figure 3.7. More simulations with plasticity results will be presented in Chapter 4.

3.3 How to combine the two models

Synaptic plasticity is highly related to the temporal order of synaptic input action potentials, either depressing (weakening) or potentiating (strengthening) output action potentials as Hebb originally postulated. In this dissertation, we want to

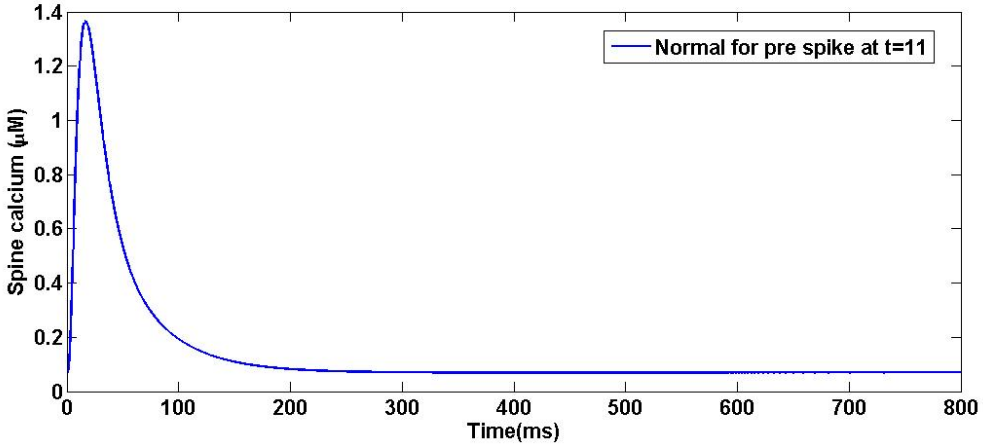

Figure 3.6. Spine calcium for pre spike only at t=11.

test whether the potentiation induced by different timings pre and post spikes under various types of stress will be different in spine calcium influx for normal and PTSD states. Also, we test the plasticity alternation under the condition of imposing an acute stress for normal and PTSD states.

To do so, we take average values of cortisol level from normal state and PTSD state. We assume all default parameters' values in Rubin model except for NMDA receptor conductance and AMPA receptor conductance, which are regulated by cortisol level. We align the values of NMDAR conductance and AMPAR conductance in Rubin model as baseline, with the average cortisol level in the normal state. For the PTSD state, we set NMDAR and AMPAR base values at 21 percent less than these of normal state. The conductance difference is calculated by averaging the peak value and the base value of $CORT$ in normal state and PTSD state respectively. We define the function P as follows:

$$P = \frac{m_{Ptsd} - m_{Normal}}{m_{Normal}} \tag{3.19}$$

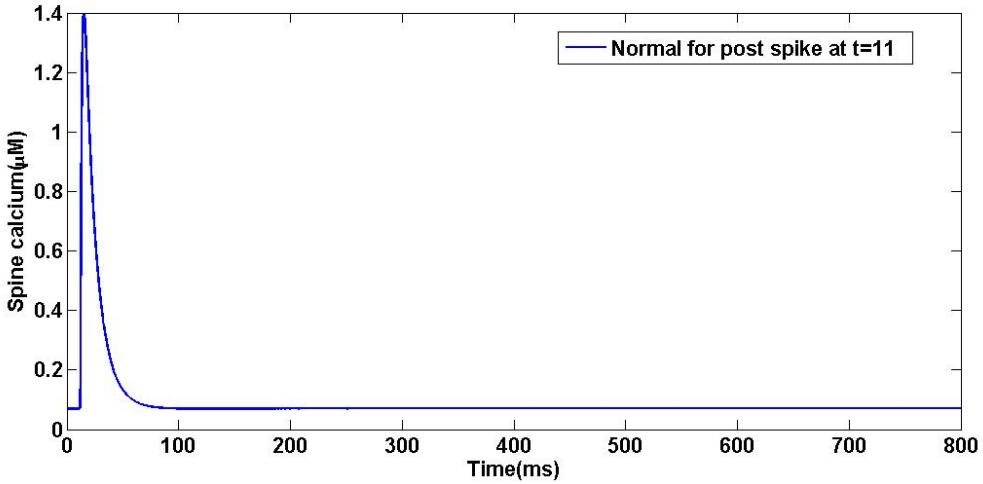

Figure 3.7. Spine calcium for post spike only at t=11.

where m_x is defined as

$$m_x = (Cortisol_{x,peak} + Cortisol_{x,base})/2 \tag{3.20}$$

and $x \in Ptsd, Normal$.

CHAPTER 4

NUMERICAL SIMULATION

4.1 Single Jump

4.1.1 Case 1: Regular Pre or Post only Spike

In order to validate the proposed new model, the system of ordinary differential equations is numerically solved using forth-order Runge-kutta method in XPPAUT [41]. The results of these comparisons between normal state and PTSD state are shown in the following.

Table 4.1. Spine voltage peak values for single presynaptic spike

State	t=1ms	t=49ms
Normal	-63.6336	-63.4751
PTSD	-65.0209	-64.9111

The first series of results show different experiments where only single presynaptic spike or postsynaptic spike are taken into account. Figure 4.1 shows that when only presynaptic spike at t=1ms, and t=49ms. Clearly we can see that spine voltage all go up in a small range for both normal state and PTSD state. Both of the cases do not get to the depolarization status to remove the magnesium block by Back Propagating action potentials (BPAP). Also, under either situations, the spine voltages go back to the resting state over 50ms. In table 4.1, we can see for both t=1ms and t=49ms, the peak value of Spine voltage for PTSD state will be slightly

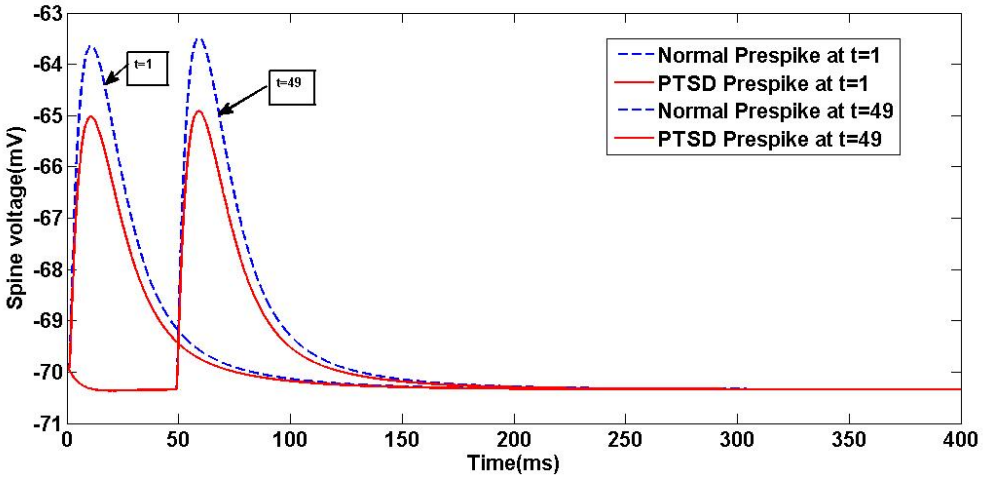

Figure 4.1. Spine voltage value in response to single presynaptic spike at t=1 and t=49 for normal state and PTSD state.

lower than that of the normal state. This is due to the average lower cortisol level for PTSD state suppresses the glutamate receptors.

Table 4.2. Spine calcium peak values for single presynaptic spikes

State	t=1ms	t=49ms
Normal	1.3657	1.3816
PTSD	0.9756	0.9826

Correspondingly in Figure 4.2, the calcium influx for normal state is slightly higher than that of the PTSD state. Although both cases have a short calcium influx during the presynaptic spike, and they all go back to the rest calcium level after 150ms, the peak levels shown in Table 4.2 are still not high enough to induce potentiation.

Next, the model is tested with a single postsynaptic spike for normal state and PTSD state. As in Figure 4.3 and Figure 4.4, for the spine voltage and spine

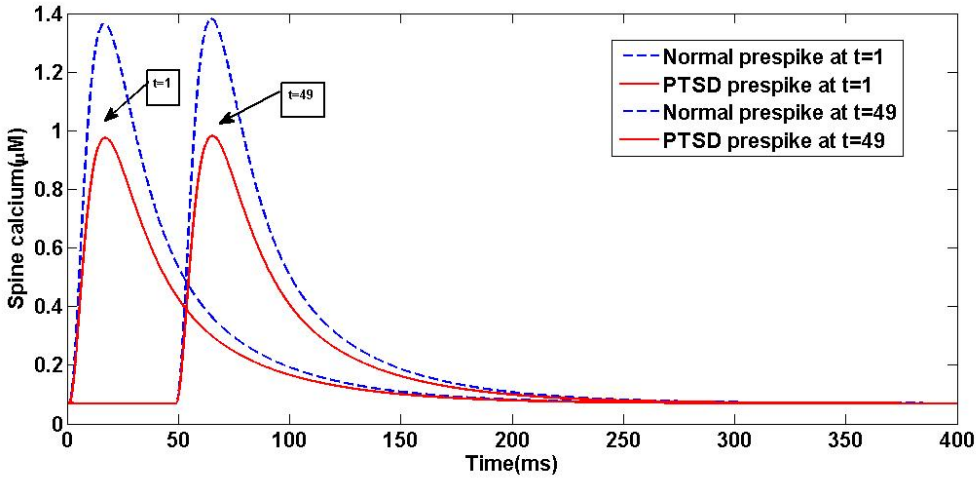

Figure 4.2. Spine calcium value in response to single presynaptic spike at t=1 and t=49 for normal state and PTSD state.

Table 4.3. Spine voltage peak values for single postsynaptic spike

State	t=1ms	t=49ms
Normal	-30.7689	-30.7689
PTSD	-30.2532	-30.2532

calcium influx, at t=1ms and 4=49ms, the results for two cases are nearly same. Compared with Table 4.1 and Figure 4.1, we observe the voltage peak levels for normal state and PTSD state induced by single postsynaptic spikes will much higher than single presynaptic spike case. However, the time intervals to go back to the rest state are much shorter (less than 5ms) than those in the single presynatpic spike input case, and in both cases the neuron do not achieve depolarization to remove the magnesium block and hence there is no potentiation. One possible reason for the peak levels with no difference with two states for postsynaptic spike is that presyanptic occurs in spine which will affect the neuron receptors glutamate transmission, by turning off the presynaptic spike, it will stay in rest state and has no interactions with postsynaptic spike. The postsynaptic input is applied directly on the soma.

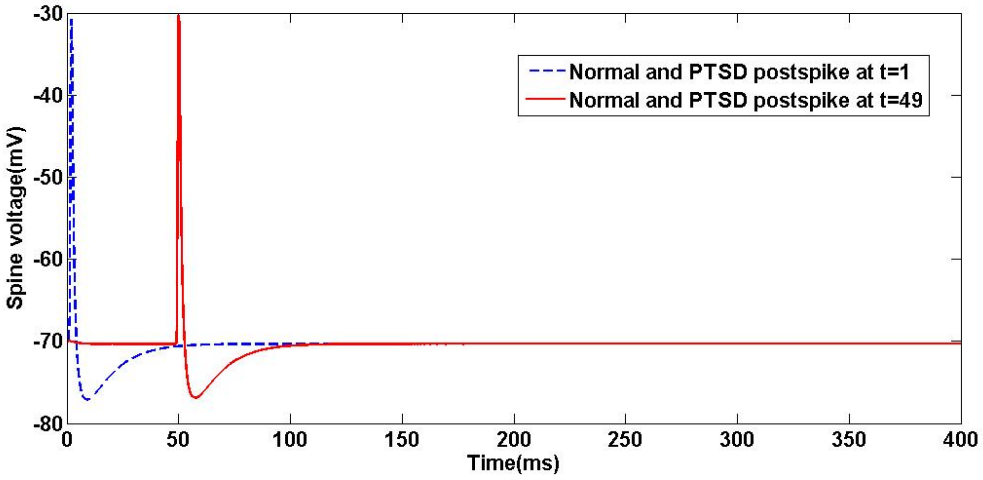

Figure 4.3. Spine voltage value in response to single postsynaptic spike at t=1 and t=49 for normal state and PTSD state.

Although the postsynaptic spike raises up a higher level compared to the presynaptic spike case, it only lasts in a very short time, and make almost no difference for the calcium peak value.

Table 4.4. Spine calcium peak values for single postsynaptic spikes

State	t=1ms	t=49ms
Normal	1.1792	1.4786
PTSD	1.1792	1.4786

4.1.2 Case 2: Continuous Pre or post spike train

In this subsection, we test the model using continuous presynaptic or postsynaptic spike train. The continuous presynaptic or postsynaptic spikes is a continuous spiking train that turns on presynaptic or postsynaptic spikes in a 900ms interval. From Figure 4.5, it is clearly shown that the spine voltages for both cases are raising

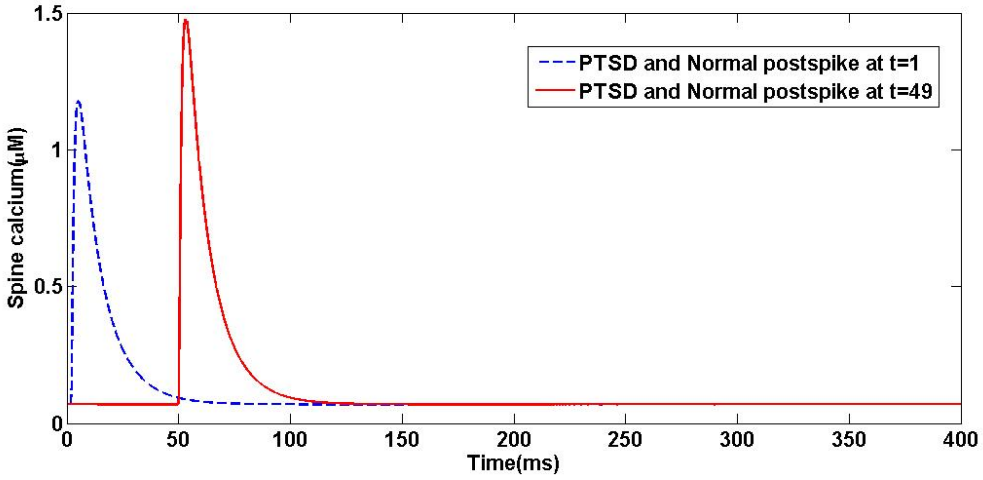

Figure 4.4. Spine calcium value in response to single postsynaptic spike at t=1 and t=49 for normal state and PTSD state.

up to a peak and then going down to the rest state in a short time (less than 35ms), then the voltages go up to be depolarized and last for a long time (over 100ms). Both cases have oscillations when returning to the rest state. The spine voltages form a periodic depolarization and hence induce the potentiation. Also, the peak level for both cases are almost the same, but there is a time delay for PTSD state compared to normal state. This is because the cortisol level difference affects the receptors (NMDA,AMPA) conductances then hence delays the depolarization time.

Table 4.5. Spine calcium peak values for continuous presynaptic spikes

State	peak value
Normal	144.2820
PTSD	130.3140

Figure 4.6 depicts the spine calcium influx for two states. It is seen that both calcium concentration will raise up as the voltages go up, and the delays also happen

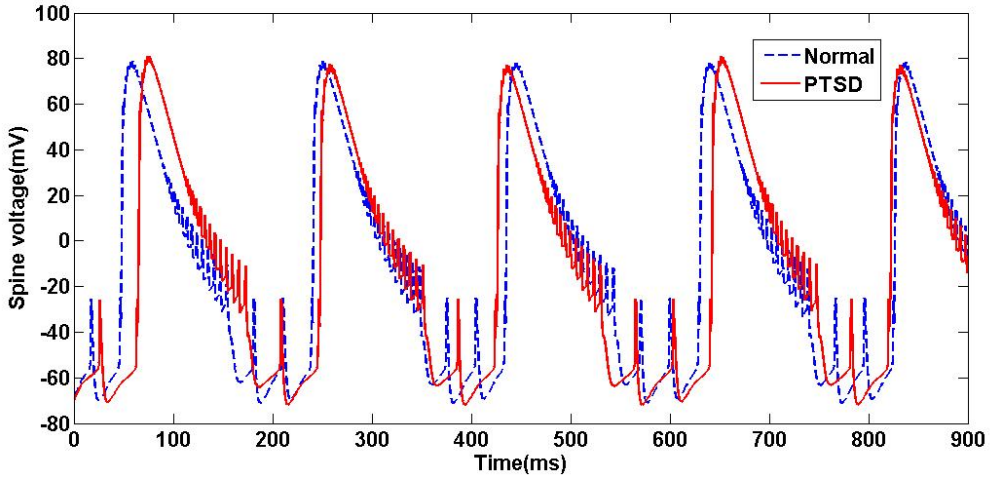

Figure 4.5. Spine voltage value in response to continuous presynaptic spikes for normal state and PTSD state.

for two different states. However, the peak calcium level for normal state (144.2820) is higher than PTSD state (130.3140). This is due to the reduced receptors' conductances reduce the activation level of the receptors in response to continuous spikes.

In Figure 4.7, under a continuous postsynaptic input train, the spine voltage will oscillate from -60mv to -40mv in a very short time, and then the voltage goes up to become depolarization. For the first 400ms, the range of voltages go from -60mv to + 45mv. Different with continuous presynaptic spike case, the voltage will lead to smaller oscillation (-35mv to 10mv) after a shorter period (less than 80ms). Correspondingly in Figure 4.8 the calcium level in spine will form second large jumps during the first 400ms, then becomes small periodic oscillation.

The simulation is done for the normal state. As we explain earlier, since presynaptic spike is turned off, no glutamate is released between two neurons, hence the receptors will keep in static state and make no influence on the calcium concentration in the spine. The case for PTSD state is similar to the normal state, and is not repeated here.

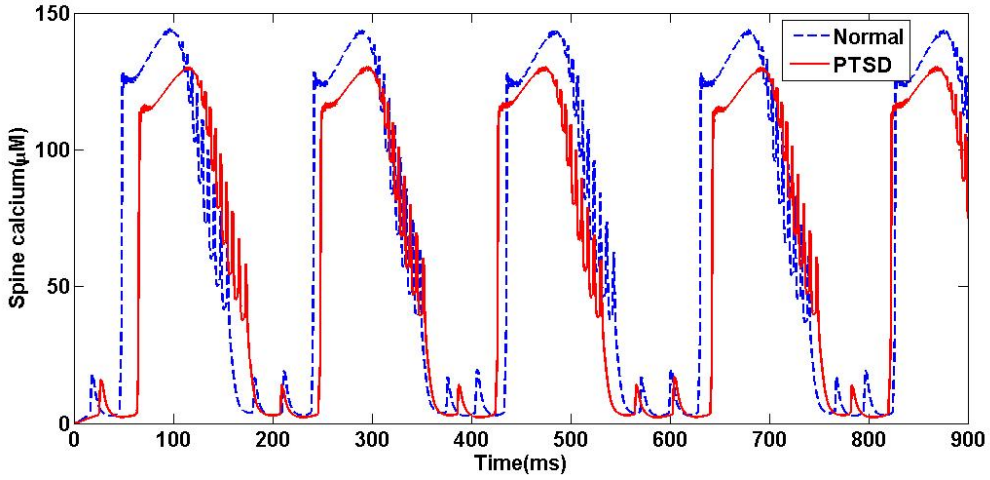

Figure 4.6. Spine calcium value in response to continuous presyanptic spikes for normal state and PTSD state.

4.1.3 Case 3: Periodic Pre or Post only Spike

In this subsection, we test the model using periodic presynaptic or postsynaptic spike, and the spike period is 300 ms , that is 3.33 Hz.

In Figure 4.9, we can see that periodic presynaptic spikes cause the spine voltage go up in a very small range (5 to 7), and voltages for both normal state and PTSD state are very close to the initial value. The peak for spine voltage after each presynaptic spike returns to the resting value around 100ms. There is no depolarization during the the periodic spikes.

Table 4.6. Spine calcium peak values for periodic postsynaptic spikes

State	t=1ms	t=49ms
Normal	1.1692	1.4798
PTSD	1.4798	1.4798

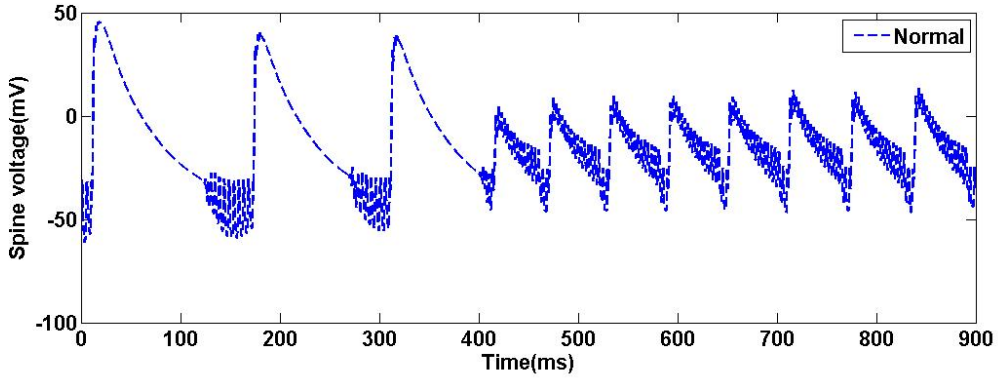

Figure 4.7. Spine voltage value in response to continuous postsynaptic spikes for normal state and PTSD state.

Figure 4.10 depict the spine calcium concentration for two states at different initial spiking time (t=1 ms, t=49 ms) separately. Since the cortisol differences between normal state and PTSD state affects the efficiency of neuron receptors during the glutamate transmission and thus changes the conductance, we observe the calcium influx in spine for normal state is higher than that of PTSD state.

However, since there is no depolarization during the periodic spikes, the calcium influx in spine only attains small peaks (less than 2μg/dL). There is no potentiation under this situation.

Figure 4.11 and Figure 4.12 are very similar with the corresponding figures of single postsynaptic spike. The only difference is that first calcium peak level differs for t=1ms and t=49ms. As the following postsynaptic spike occurs, the calcium peak level and spine calcium peak level will become stable. For both cases of periodic postsynaptic spikes input, the spine voltages do not induce depolarization, and the calcium levels only raise in a very small range and then return to the rest state.

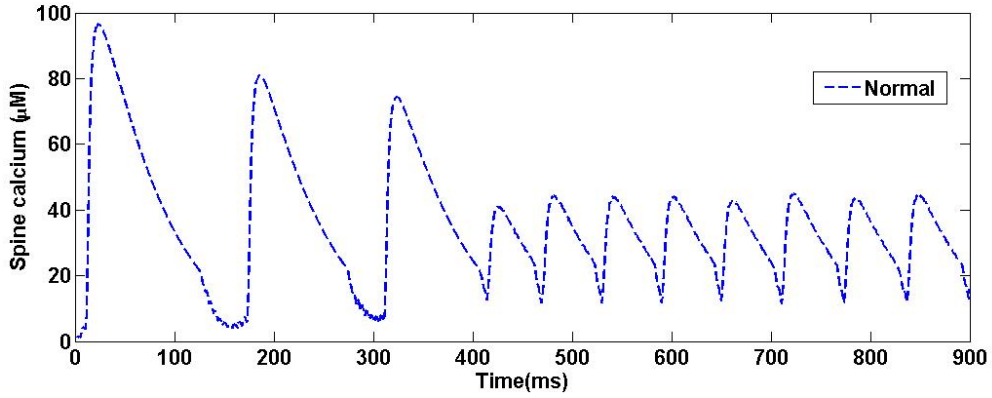

Figure 4.8. Spine calcium value in response to continuous postsynaptic spikes for normal state and PTSD state.

From the first six testing cases, we attain the conclusion that presynaptic spike will play a much important role for inducing the potentiation. However, without considering the paired spikes, we still can not get the full understanding about the Spike Time Dependent Plasticity (STDP).

4.2 Pair Jump

4.2.1 Case 1: Regular Pre-Post and Post-Pre Spike

Pre-delta-post spikes stand for the presynaptic spike happens first, after delta ms, the postsynaptic spike will come out. Post-delta-pre spike is the reverse version of pre-delta-post, the presynaptic spike follows a postsynaptic spike after a delta ms.

Figure 4.13 depicts results for single pre-delta-post spikes at different delta values (2, 10, 20, 30, 40, 50). From the Figure 4.13, we can clearly see that the peak level of the calcium is going higher for $0ms < delta \leq 20ms$, after that it drops down as delta becomes larger. The large influx of the Calcium goes into spine since

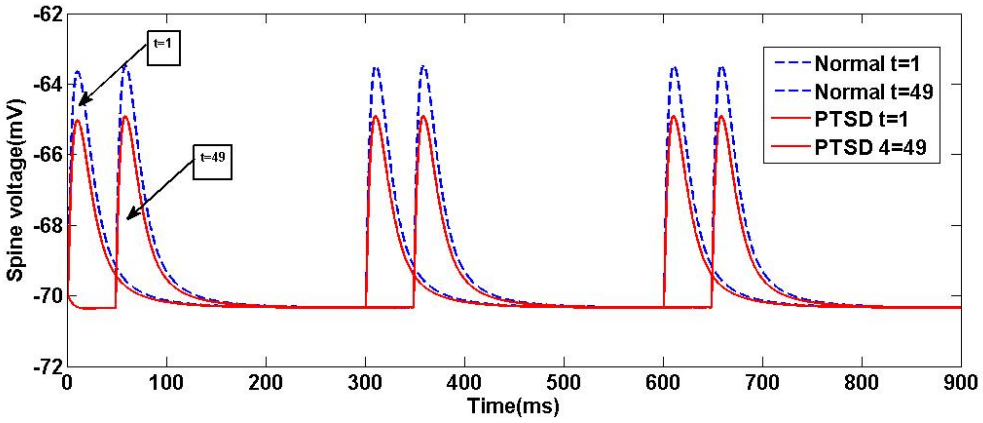

Figure 4.9. Spine voltage value in response to periodic presynaptic spikes for normal state and PTSD state.

the magnesium block was removed. However, as delta becomes bigger, the influx of calcium will reduce since the BPAP at the spine comes later.

In Figure 4.14, which depicts results for single post-delta-pre spikes, we see that all the peak levels for calcium influx are much lower than those of in Figure 4.13. Also, we find that for all post-delta-pre cases except when delta is equal to 2 approximately, the calcium influx forms two peaks. As delta becomes bigger, the formed second peak will become higher compared to the first peak.

This also satisfies the Spike Timing-Dependent Plasticity rule, i.e, in the pre-delta-post spike, the calcium level in spine will touch a level ($>4\mu$g/dL) that will induce potentiation. However, the post-delta-pre spikes will only induce depression since the peak level of calcium in spine is lower than 1.5μg/dL.

Figure 4.15 shows the peak levels for pre-delta-post where delta takes from -50 to 50. We can see the shape of peak level of the calcium accords well with the results from Bi and Poo [32] in graph 2.5 when delta is greater than 0. For the situation

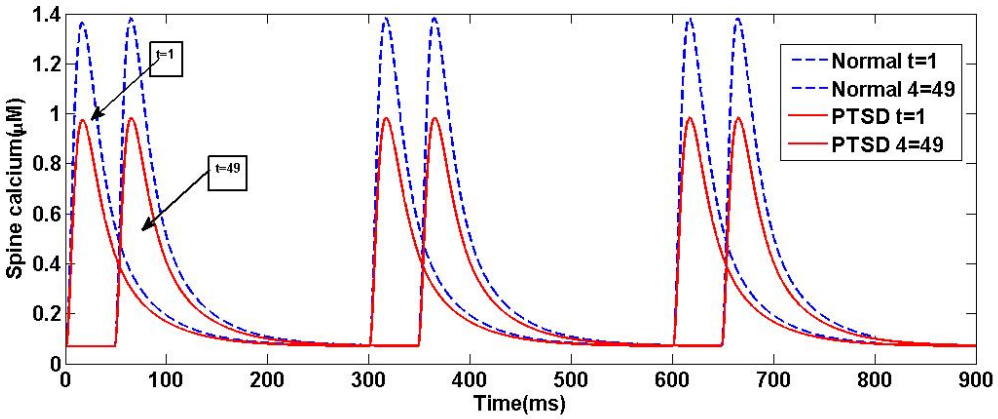

Figure 4.10. Spine calcium value in response to periodic presyanptic spikes for normal state and PTSD state.

delta is less than 0, the growth rate as delta decreases is not as much as the typical STDP results [32].

4.2.2 Case 2: Continuous with periodic Pre-Post and Post-Pre Spike

In this subsection, first we want to test if we incorporate a continuous presynaptic input and one periodic postsynaptic spike, whether the plasticity for two states will still hold the results as the results shown in the previous cases. Since this case may be difficult to test experimentally, we only show the calculated results and discuss the variability.

Figure 4.16 is the spine calcium peak value for this composed pre-delta-post spike. We can see that spine calcium peak level in normal state is higher than that of PTSD state. When delta is smaller than 0 and greater than -5, the calcium peak level is not strictly decreasing. Also, when the delta value is greater than 10, the calcium peak value keeps the similar high level until delta equals 50. This result does not fit in the classic STDP results in the literature [32]. There are some plausible opinions

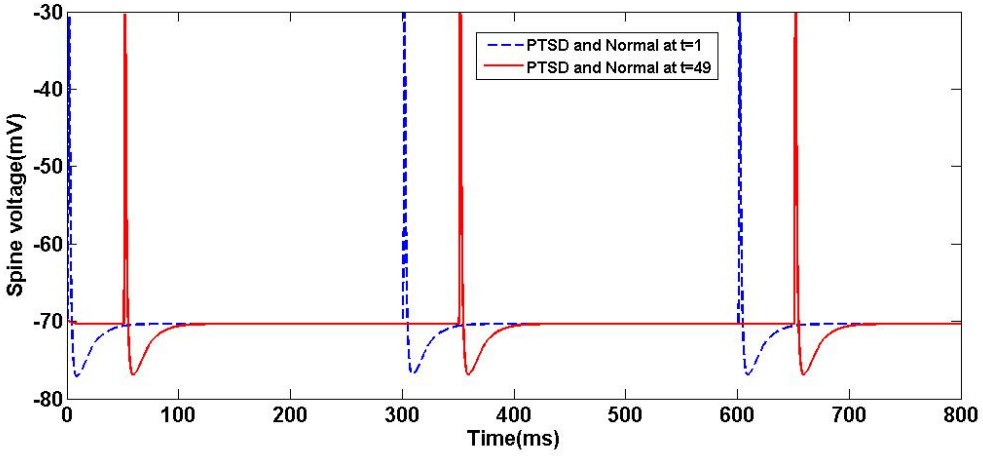

Figure 4.11. Spine voltage value in response to periodic postsyanptic spikes for normal state and PTSD state.

that can explain: (i): Calcium Peak Level is one type biomarker for synapse plasticity and it is not the only one; (ii): under the condition of continuous presynaptic input, the glutamate is continuously released, hence it might lead to potentation into a saturation level, which might lead the calcium peak level stays same.

To continue the test under this composed pre-delta-post stimulation, we then calculate the average calcium in the spine at different time intervals (900ms, 9000ms). Figure 4.18 shows the spine calcium average value over 900 ms, and the value normal state is higher than that of PTSD state. Both average values are not very stable for delta from -50 to 50 due to calcium oscillation, and they do not reflect the property of STDP trend.

However, the results over 9000ms is average surprising. In Figure 4.20, the average value for PTSD state is very stable compared to normal state. But when delta is less than 0, the average calcium value for normal state is higher than the case when is greater than 0. This result does not fit the shape of STDP totally.

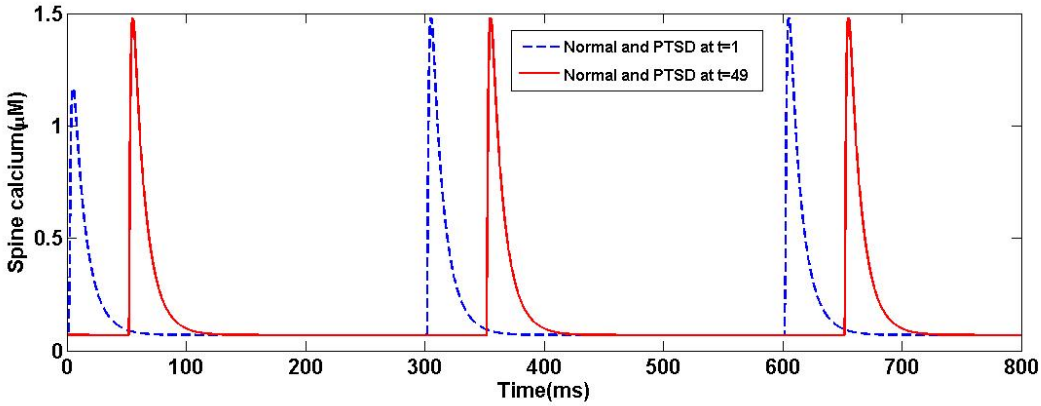

Figure 4.12. Spine calcium value in response to periodic postsyanptic spikes for normal state and PTSD state.

In the second part of this subsection, we will set the postsynaptic spike as a continuous input, and the presynaptic spike will be a periodic spike train which has a period of 300ms. Figure 4.17 depicts the spine calcium peak values in a 900ms for delta is between -50 to 50. Clearly we see that overall calcium peak values when $-50 \leq delta < 0$ is higher than these of $0 \leq delta \leq 50$. Also, the left side of this graph is less oscillating than the right side. Compared to the reverse pre-delta-post spike inputs in Figure 4.16, still the calcium value in normal state is higher than that of in PTSD state. However, the right side of Figure 4.16 will be more flat than that of in Figure 4.17. The overall peak values in Figure 4.17 are lower than that of in Figure 4.16. The result in Figure 4.17 does not satisfy the shape of typical STDP.

Next, we also calculate the average calcium in the spine at different time intervals (900ms, 9000ms). In Figure 4.19, it shows the average calcium value in a 900ms interval. Compared with the reversed case in Figure 4.18, the average values for both normal state and PTSD state are lower than these of in Figure 4.18, but the value

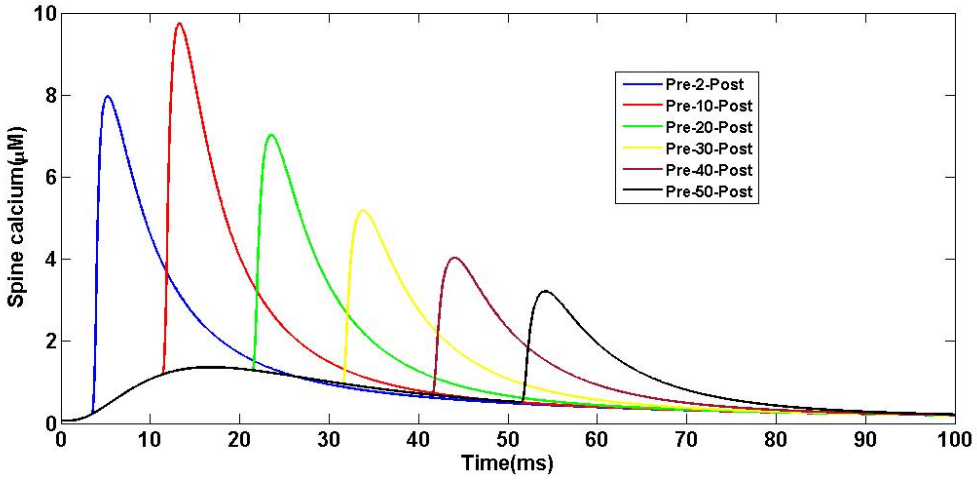

Figure 4.13. Spine calcium value in response to regular pre-delta-post spike inputs at normal state.

difference between two states are much smaller in Figure 4.19. Also, left side of Figure 4.19 are all higher than that of right side, while the Figure 4.18 is more flat.

Figure 4.21 depicts the average calcium value in 9000ms interval when we set a continuous postsynaptic spike inputs and a periodic presynaptic spikes. Different with the reversed spike case in Figure 4.20, the calcium average values for normal state are higher than these of in PTSD state. Also, the difference between average values for two states is small compared to the situation shown in Figure 4.20.

To summarize, the testing results for the composed spikes are not ideal for the protocol. Although most of the cases showed the expected calcium difference between normal state and PTSD state, however the results are not following a STDP governing rule that can describe clearly for the plasticity difference under different timing condition.

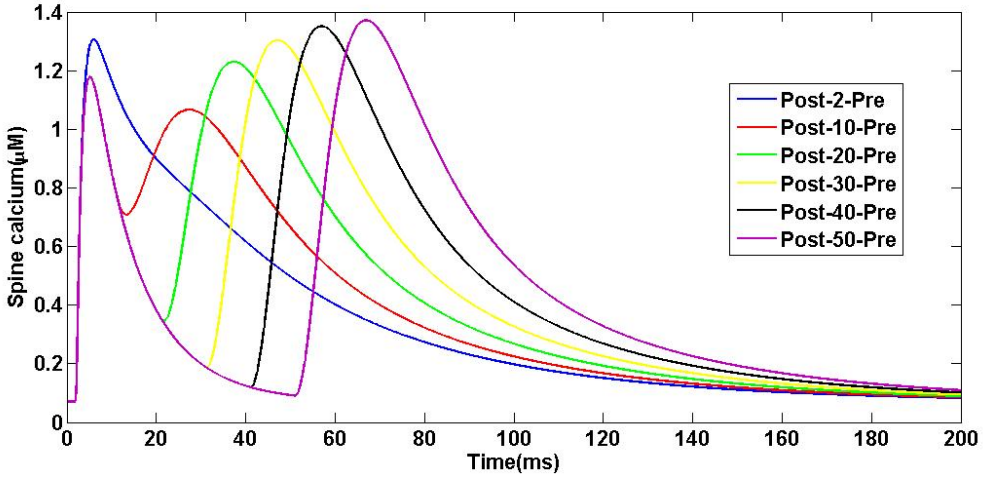

Figure 4.14. Spine calcium value in response to regular post-delta-pre spike inputs at normal state.

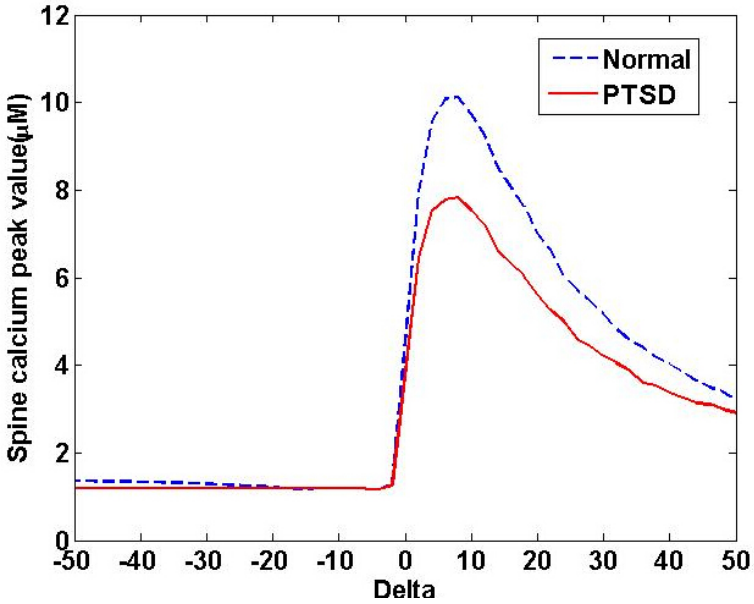

Figure 4.15. Spine calcium peak values in response to regular pre-delta-post spike inputs as a function of the timing difference delta.

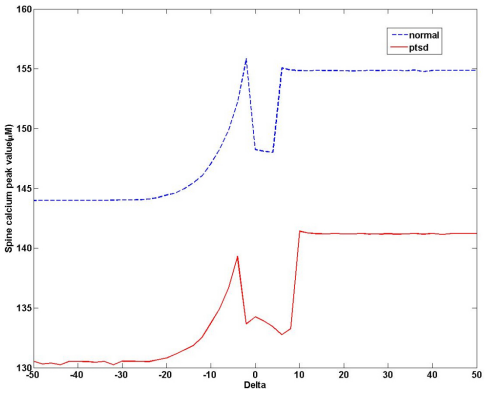

Figure 4.16. Spine calcium peak values in response to composed pre-delta-post spikes as a function of the timing difference delta.

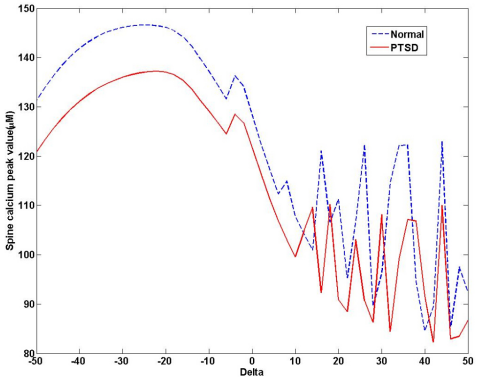

Figure 4.17. Spine calcium peak values in response to reversed composed pre-delta-post spikes as a function of the timing difference delta.

4.2.3 Case 3: Periodic Pre-Post and Post-Pre Spike

In the last subsection of this chapter, we test our model in periodic pre-delta-post spikes in different periods (300ms, 100ms). In Figure 4.22, which depicts the results for periodic pre-delta-post spikes at a period of 300ms, the calculation indicated that calcium peak level in spine for delta ranging from -50 to +50 is very similar to single pre-delta-post spike shown in Figure 4.15. The result fits the shape of STDP very well for the right half part, the decreasing rate for the left side is more flat compared to that of in Figure 2.5.

For the spike input period of 100ms, the result is in Figure 4.23. Compared to Figure 4.22, it can be seen that the calcium peak values in Figure 4.23 is all higher (almost 2μg/dL) than Figure 4.22. Because of the spike frequency is 10 Hz in presynaptic and postsynaptic spikes, that is three times of the original one. It acts on the activation level of these receptors, mainly reduces the activation level to make it easier to get depolarization. Hence the calcium influx peak will become higher in this case. Cortisol difference will still make the calcium peak level for normal state is higher than that of PTSD state.

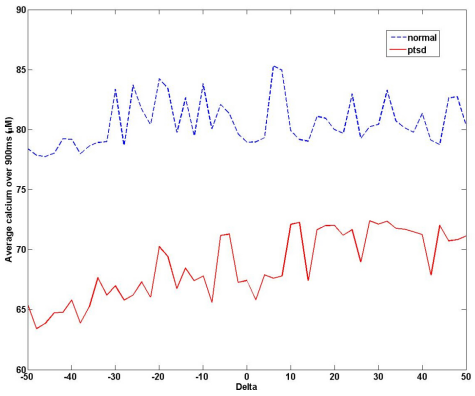

Figure 4.18. Spine calcium average value in response to composed pre-delta-post stimulation in 900ms.

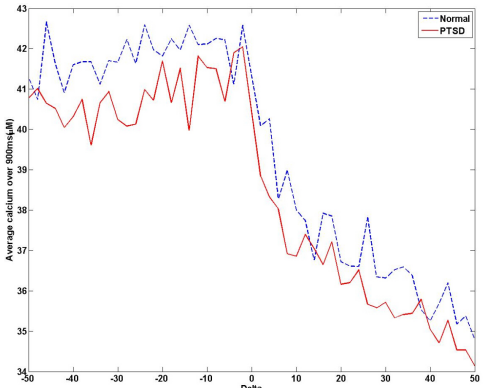

Figure 4.19. Spine calcium average value in response to reversed composed pre-delta-post stimulation in 900ms.

Also, the calcium peak value in Figure 4.23 is higher than that of in Figure 4.22 for every delta value. For the post-delta-pre part, the calcium level is between 2μg/dL and 4μg/dL. This interval is also called the decision interval, since based on the following spikes input, it either become potentiation or depression. We can see that raising the frequency of periodic spikes will improve the overall possibility of inducing potentiation.

4.3 Acute stress imposed dynamics

4.3.1 Cortisol dynamics with acute stress

To test the cortisol dynamics for normal state and PTSD state with an imposed acute stress (4 hours in duration), we design our experiment as follows:

Add one acute stress function $f_{acute}(t)$ into K_{stress} in equation 3.1, and $f_{acute}(t)$ is defined as follows:

$$f_{acute}(t) = H(t - delta) * H(delta + 4 - t) \tag{4.1}$$

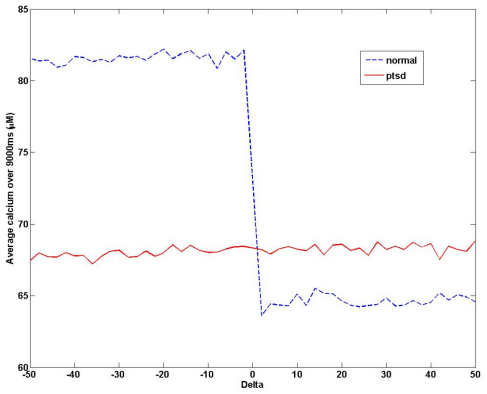

Figure 4.20. Spine calcium average value in response to composed pre-delta-post stimulation in 9000ms.

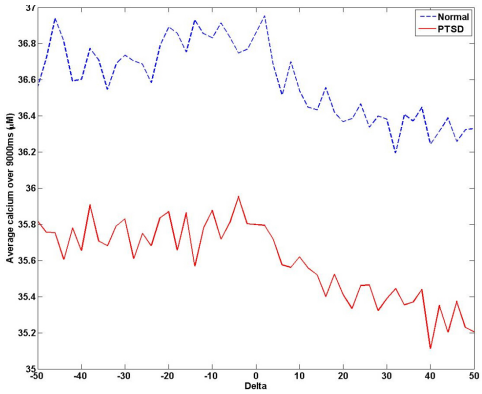

Figure 4.21. Spine calcium average value in response to composed pre-delta-post stimulation in 9000ms.

where $H(x)$ is heaviside step function, *delta* stands for the time where we impose the acute stress.

Figure 4.24 shows the result of $CORT$ by imposing an 4 hours acute stress to normal state and PTSD state. Clearly we can see the acute stress induce higher concentration level of cortisol for normal state and it takes more than 30 hours to get back to regular periodic secretion. However, cortisol level of human with PTSD state under acute stress only increases very small for its peak and period changes not much.

In this section, we average the cortisol concentration under acute stress condition to test the plasticity difference between normal state and PTSD state.

We use the measure method for the acute stress case. Different from the normal state and PTSD state without acute stress, the acute stress situation affects the cortisol secretion period: a normal state takes almost 35 hours to return normal 24 hours period; for a PTSD subject, the change of period is not that much (about 26 hours). So we define one ratio function q as follows:

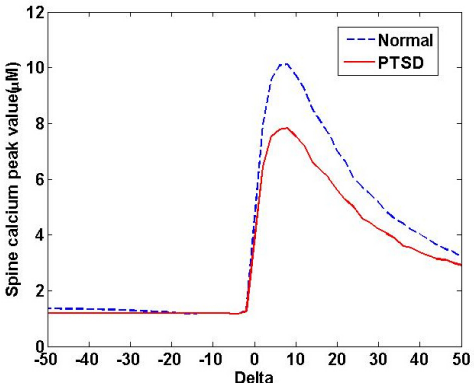

Figure 4.22. Spine calcium peak values in response to periodic(300ms) pre-delta-post spikes as a function of the timing difference delta.

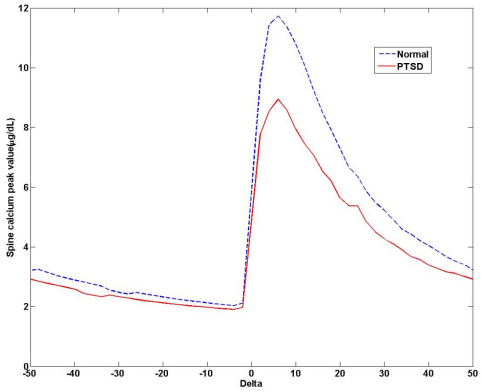

Figure 4.23. Spine calcium peak values in response to periodic(100ms) pre-delta-post spike as a function of the timing difference delta.

$$q(x) = \frac{A_x - A_{normal}}{A_{normal}} \tag{4.2}$$

where A_{normal} is the average cortisol concentration in 24 hours, $x \in normal, ptsd$ under acute stress condition and A_x is the average cortisol concentration in its corresponding acting period (35 hours and 26 hours).

The following are the computational results:

$$q(normal) = \frac{19.2031 - 12.2103}{12.2103} = 57.3\% \tag{4.3}$$

$$q(ptsd) = \frac{10.37 - 12.2103}{12.2103} = -15.1\% \tag{4.4}$$

4.3.2 Periodic Spikes results

From the above results, we can clearly see that the periodic pre-delta-post spikes reveal the STDP more accurately than other cases, and periodic spikes are more close to the experiments. In this subsection, we test the model using different periodic spikes for the acute stress imposed situation. As for the periodic spikes, we generate

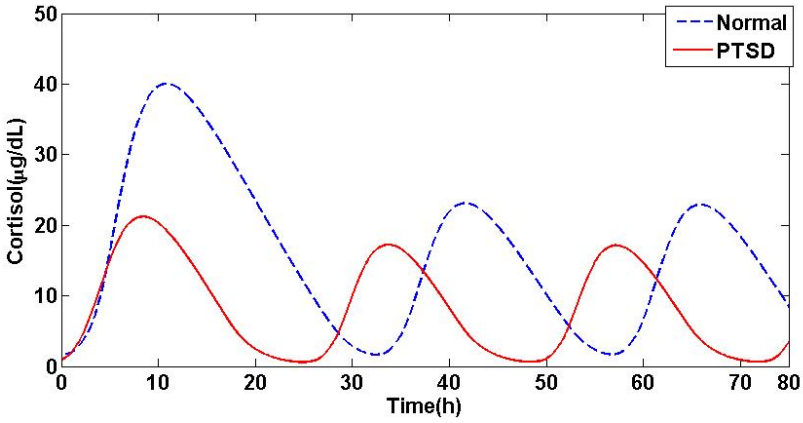

Figure 4.24. The cortisol level under an imposed 4 hours(t=3 to t=7) acute stress. The normal state is depicted in dashed line, and the PTSD state is depicted in solid line.

the spike input periodically with a period (300ms, 100ms, 33ms). We verify that the shape of calcium influx in spine will display periodically after the first or the second pair spikes' for the model.

In Figure 4.25, we can see that for the pre-2-post spikes with a period of 300ms for normal human with an imposed acute stress, the calcium level in spine will go up around 17.1297 μg/dL, then it returns to steady state until another paired spikes comes in the next 300 ms. However, starting from the pre-4-post spikes, until pre-18-post spikes, the calcium peak level jumps to around 140 μg/dL and lasts almost 150ms when the second periodic spikes comes. Due to the high cortisol concentration induced by a 4 hours acute stress, it improves the NMDA and AMPA receptors' conductances. In another word, the threshold levels of these receptors for depolarization become lower, and thus it can accumulate to a much higher calcium influx. The time duration for higher level calcium is almost 150ms.

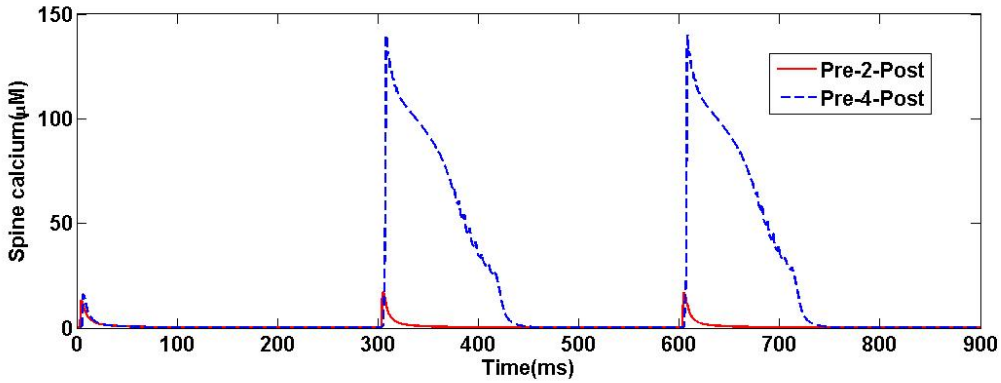

Figure 4.25. Spine calcium influx for pre-2-post and pre-4-post for normal state.

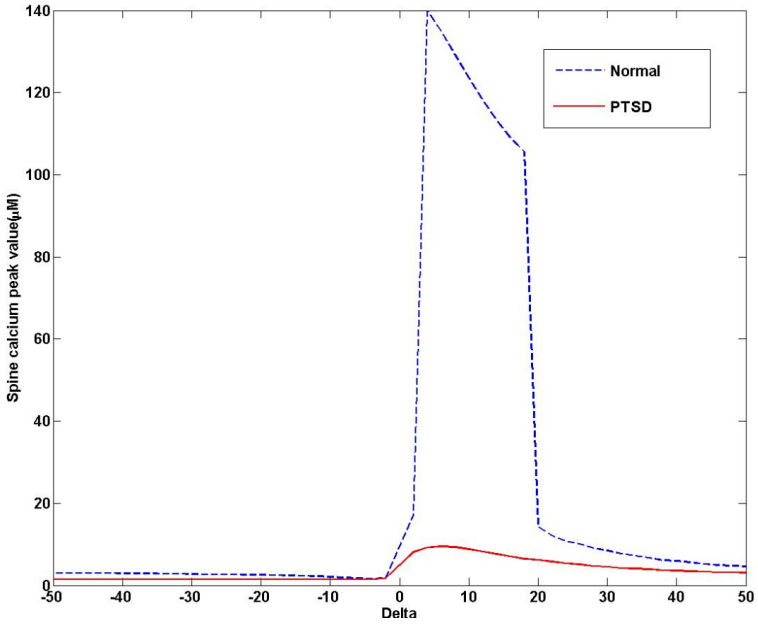

Figure 4.26. Spine calcium peak values in response to a 300ms periodic spikes as a function of the timing difference delta.

Figure 4.26 and Figure 4.27 depict Calcium peak values for 300ms and 100ms periodic spikes. Two graphs are very similar except in the 100ms case, there exists a small oscillation between 15 to 20. The acute stress imposed on human in normal state plays an more significant role for the induction of potentation compared to human in PTSD state. This is due to the high concentration secretion in cortisol regulates the receptors' conductances and the activation level.

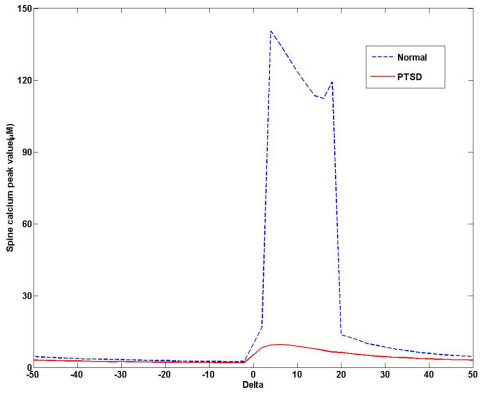

Figure 4.27. Spine calcium peak values in response to a 100ms periodic spikes as a function of the timing difference delta.

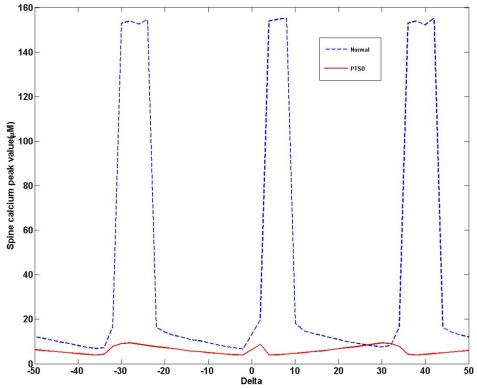

Figure 4.28. Spine calcium peak values in response to a 33ms periodic spikes as a function of the timing difference delta.

Figure 4.28 is the Calcium peak value when we test our model in a 33ms periodic spike. For a 100 domain, clearly it can be seen that peak level is also a 33ms periodic oscillation. Compared to Figure 4.26 and Figure 4.27, a higher frequency will short the super high level calcium for normal state. Still for PTSD state, the acute stress imposed does not affect too much for the calcium peak value.

CHAPTER 5

CONCLUSION AND FUTURE WORK

In this dissertation, we focused on the relationship between cortisol secretion level and the effects of corresponding synapse plasticity for human in normal state and PTSD state.

We first introduced, in Chapter 2, the theoretical key points of designing our model, i.e, assuming glucocorticoid as the main biomarker to distinguish healthy people with people in PTSD, and also choosing calcium influx change in spine as the significant marker for synapse plasticity change, and also we present the importance of this research. In Chapter 3, we present a model that connected glucocorticoid dynamics related with stress response and two compartments CA1 neuron model. Based on the experimental results and model construction supports shown in Chapter 2, we presented the necessary condition in the model for the synapse change corresponding to variance of stress. Also, we investigated numerically the two parameters Hopf bifurcation analysis for the HPA model. Our analysis showed that certain key parameters, such as the stress indicator K_{stress}, CRH degradation rate V_{s3}, and ACTH degradation rate V_{s4}, play a crucial role in describing the complexity of glucocorticoid dynamics for normal state and PTSD state.

In chapter 4, we tested our model under different type of spikes. For the single jump section, the results show that no matter which type of single spike input was applied to our model, calcium values for PTSD state are all smaller than that of normal state. The situation of single spike and periodic single spike are very similar and both cases do not induce potentation as the starting spiking time varies. For

the single continuous input, potentiations are induced and the average spine calcium levels are higher for continuous presynaptic spike. Also, for all cases in single jumps, the differences of calcium influx in spine is bigger under single presynaptic spike inputs. For the pair jump section, the calcium peak levels for single pre-delta-post and 300ms periodic pre-delta-post are very similar. The calcium peak value will be increased as the period decreases to 100ms. Both of these two cases agree with STDP protocol [32]. For the composed pair jumps section, most of the calcium values for normal state are higher than that of PTSD state. The results do not support STDP and the results are fluctuated with delta changes. As for the acute stress imposed section, high level of glucocorticoid concentration associated with delayed period was found for normal state in our simulation. For different periodic pre-delta-post spikes, higher calcium peak levels were observed in normal state when delta is between 0 and 20 compared to that of in PTSD state, which also agree with STDP protocol.

In the appendix, we presented a theoretical GR included HPA model termed Extended Minimal Model (EMM). We proved the the basic properties of our model including existence and uniqueness of solutions for initial value problems, non negativity of solutions, the existence and uniqueness of equilibrium, a trapping region, and stability analysis of equilibrium points.

In conclusion, the mathematical model of PTSD and algorithm are capable to systematically test synaptic plasticity variance in PTSD states. This model can help to find multiple cortisol dynamics and potentiation/depression patterns of PTSD. Our preliminary date presented here shows the feasibility of our model as a predictive tool for studying some aspect of PTSD and its related effects on brain memory and learning functions. Certainly, the conducted test here reflects only one measure for STDP. Further investigation is needed for measuring the effects of PTSD on STDP as well as LTP in general.

As a future work, we propose to generalize the model to people with different types of stress disorder. Different cortisol levels related to different stress disorder contribute to a main factor for memory degeneration, but age is another considerable factor to neuron plasticity. Also, investigating the results under the triplets presynaptic and postsynaptic spikes will be helpful to fully understand the brain function of our model. Exploring these ideas might lead similar models with additional features added, and the parameters of the model can be most likely measured in neuroscience experiments. A more comprehensive study of this model will provide a better understanding of many applications of neuron models in neuroscience.

APPENDIX A

EXTENDED MINIMAL HPA MODEL

In this appendix, we present a detailed proof of our extended minimal HPA model.

A.1 Extended Minimal model

Vinther et al. (2011) first gave out the definition of minimal model based on the widely accepted mechanisms that negative feedback from cortisol on CRH and ACTH. The work done by Gupta el al. (2007) and Sriram el al. (2011) show that with the consideration of GR in the HPA axis, more characteristics about the HPA axis are revealed based on early experimental data by Yehuda et al (1996) and LJ Crofford et al (2004). In our term extended minimal model, we consider our network of cortisol in HPA axis with the GR and we assume the negative feedback are from GR to CRH and ACTH.

A.1.1 Build the model

First, we introduce the assumtions of the extended minimal model. A positive stimulation, e.g. stress for hypothalamus with a constant rate m_1 on the concentration of CRH ($y1$) is stimulated. CRH activates the secretion of ACTH ($y2$) with a constant rate m_2 and ACTH stimulates the secretion of cortisol ($y3$) with one constant rate m_3. Cortisol has a constant rate m_4 function on GR ($y4$). The concentrations of CRH, ACTH,cortisol and GR are depleted through n_1,n_2, n_3 and n_4. Our modeling set the negative feedback from the concentration of GR on the concentration of CRH and ACTH as functions that decrease the positive stimulation on the concentration of

GR is increased. Let $f_1(y_4)$ denote the negative feedback from GR and $f_2(y_4)$ be the negative feedback from GR on ACTH. Then we can carry out the system as follows:

$$\frac{dy_1}{dt} = m_1 f_1(y_4) - n_1 y_1 \tag{A.1}$$

$$\frac{dy_2}{dt} = m_2 f_2(y_4) y_1 - n_2 y_2 \tag{A.2}$$

$$\frac{dy_3}{dt} = m_3 y_2 - n_3 y_3 \tag{A.3}$$

$$\frac{dy_4}{dt} = m_4 y_3 - n_4 y_4 \tag{A.4}$$

To simplify the model, we denote $g_1(y_4) = m_1 f_1(y_4)$ and $g_2(y_4) = m_2 f_2(y_4)$. Then the more general system of differential equations are buit as follows:

$$\frac{dy_1}{dt} = g_1(y_4) - n_1 y_1 \tag{A.5}$$

$$\frac{dy_2}{dt} = g_2(y_4) y_1 - n_2 y_2 \tag{A.6}$$

$$\frac{dy_3}{dt} = m_3 y_2 - n_3 y_3 \tag{A.7}$$

$$\frac{dy_4}{dt} = m_4 y_3 - n_4 y_4 \tag{A.8}$$

with conditions:

1. $n_1, n_2, n_3, n_4 > 0$

2. $g_1, g_2 : \mathbf{R}_+ \cup \{0\} \rightarrow \mathbf{R}_+ \cup \{0\}$, $g_1, g_2 \in C^1$, $g_1(0) > 0$, $g_2(0) > 0$
3. $\sup(g_1(y4)) = M_1$, $\sup(g_2(y4)) = M_2$, $\inf(g_1(y4)) = L_1$,$\inf(g_1(y4)) = L_2$

Since the concentration of GR affinitied by cortisol will never be negative, so the domain of two functions g_1 and g_2 will be non-negative. Also the fact that positive actives will never be negative assures the range of g_1 and g_2 will be positive. The reason we set boundary for g_1 and g_2 are based on the common sense of the body hormones. Furthermore, based on the negative feedback properties in HPA axis, we can get $g_1'(y4) < 0, g_2'(y4) < 0$, $\forall y_4 \in \mathbf{R}_+ \cup \{0\}$.

A.1.2 Basic properties about the EMM equation system

A.1.2.1 Existence and Uniqueness of solutions

Based on fundamental existence and uniquenss theorem, with the condition of $g_1, g_2 \in C^1$ and non-negative initial conditions, the system of ODE above will have a unique solution.

A.1.2.2 Non-negative solution

For each differential equation in the system, there is only one negative term $-m_i y_i$. Therefore $x_i = 0$ and $x_j \geq 0$ will lead that $\frac{dy_i}{dt} \geq 0$ for $i \neq j$. This will ead that any non-negative intinal values leads to non-negative solution for sure.

A.1.2.3 Existence and Uniquess of Equilibrium

Solving for the system $dY = 0$ and we have

$$y_1 = \frac{g_1(y_4)}{n_1} \tag{A.9}$$

$$y_2 = \frac{g_1(y_4)g_2(y_4)}{n_1 n_2} \tag{A.10}$$

$$y_3 = \frac{m_3 g_1(y_4)g_2(y_4)}{n_1 n_2 n_3} \tag{A.11}$$

$$y_4 = \frac{m_3 m_4 g_1(y_4)g_2(y_4)}{n_1 n_2 n_3 n_4} \tag{A.12}$$

Since y_1, y_2, y_3 are all based on y_4, then existence and uniqueness of y_4 will lead out the existence and uniqueness of equilibrium for this system.

Now define function

$$p(y_4) \equiv y_4, \forall y_4 \geq 0, \tag{A.13}$$

and

$$q(y_4) \equiv \frac{m_3 m_4 g_1(y_4)g_2(y_4)}{n_1 n_2 n_3 n_4}, \forall y_4 \geq 0. \tag{A.14}$$

Since $g_1(y_4)$ and $g_2(y_4)$ are all bounded and decreasing for any $y_4 \geq 0$, then $q(y_4)$ must be bounded in the interval $(0, \frac{m_3 m_4 M_1 M_2}{n_1 n_2 n_3 n_4}]$ and decreasing. Also $p(y_4)$ increases linearly and $p(0) = 0$, this assure that there will one unique y_4 exists and hence the whole system exists one unique equilibrium.

A.1.2.4 Trapping Region

For $y_1 = \frac{M_1}{n_1}$, $\frac{dy_1}{dt} \leq 0$. For $y_1 = \frac{L_1}{n_1}$, $\frac{dy_1}{dt} \geq 0$. This shows that $[\frac{L_1}{n_1} \ ; \ \frac{M_1}{n_1}]$ is a trapping region for y_1. Use similar analysis, we can get that for $y_1 \in T_1 \equiv [\frac{L_1}{n_1} \ ; \ \frac{M_1}{n_1}]$, trapping region of y_2 is $T_2 \equiv [\frac{L_1 L_2}{n_1 n_2} \ ; \ \frac{M_1 M_2}{n_1 n_2}]$. For $y_1 \in T_1$ and $y_2 \in T_2$, the trapping region of y_3 is $T_3 \equiv [\frac{m_3 L_1 L_2}{n_1 n_2 n_3} \ ; \ \frac{m_3 M_1 M_2}{n_1 n_2 n_3}]$. For $y_1 \in T_1$, $y_2 \in T_2$ and $y_3 \in T_3$, the trapping region for y_4 is $T_4 \equiv [\frac{m_3 m_4 L_1 L_2}{n_1 n_2 n_3 n_4} \ ; \ \frac{m_3 m_4 M_1 M_2}{n_1 n_2 n_3 n_4}]$.

Denote $T \equiv T_1 \times T_2 \times T_3 \times T_4$, and T is our trapping region for this system. And all the equilibrium points are in this trapping region.

A.1.2.5 Stability of equilibrium points

The unique equilibrium point in the system only can be stable or unstable.We will use the Routh Hurwitz Criteria to analyze the stability of the equilibrium points.

Routh Hurwitz Criteria for Nonlinear System

Give

$$\dot{x} = f(x), f : R_4 \to R_4, x(t_0) = x_0 \tag{A.15}$$

Suppose $\mathbf{x_s}$ is the equilibrium point of above equation and the characteristic polynomial at the equilibrium point is :

$$\lambda^4 + a_1\lambda^3 + a_2\lambda^2 + a_3\lambda + a_4 = 0 \tag{A.16}$$

If $a_1 > 0, a_2 > 0, a_3 > 0$ and $a_1 a_2 a_3 > a_3^2 + a_1^2 a_4$, then the equilibrium point is asymptotically stable. Otherwise it is unstable.

The Jacobian of the simplified system evaluated at the steady state is ,

$$\mathbf{J} = \begin{pmatrix} -n_1 & 0 & 0 & g_1'(y_4) \\ g_2(y_4) & -n_2 & 0 & y_1 g_2'(y_4) \\ 0 & m_3 & -n_3 & 0 \\ 0 & 0 & m_4 & -n_4 \end{pmatrix}.$$

The characteristic polynomial has coefficients

$$a_1 = n_1 + n_2 + n_3 + n_4 \tag{A.17}$$

$$a_2 = n_1 n_2 + n_3 n_4 \tag{A.18}$$

$$a_3 = n_1 n_2 (n_3 + n_4) + n_3 n_4 (n_1 + n_2) + (n_1 + n_2)(n_3 + n_4) - m_3 m_4 y_1 g_2'(y_4) \tag{A.19}$$

$$a_4 = n_1 n_2 n_3 n_4 - (n_1 y_1 g_2'(y_4) + g_1'(y_4) g_2(y_4)) m_3 m_4 \tag{A.20}$$

Since $n_1, n_2, n_3, n_4 > 0$ and $g_2'(y_4) < 0$, then $a_1, a_2, a_3 > 0, a_4 > 0$.

it proves there exist bounded solutions that are not equilibriums.

REFERENCES

[1] SM. Smith, WW. Vale, *The role of the hypothalamic-pituitary-adrenal axis in neuroendocrine responses to stress.* Dialogues in Clinical Neuroscience. 8(4):383-395 (2006).

[2] D. Savic, S. Jelic, N. Buric, *Stability of a general delay differential model of the hypothalamopituitary- adrenocortical system.* Int J Bifurcation chaos. 16:3079-3085 (2006).

[3] H. Besedovsky, G. Chrousos, AD. Rey, *The hypothalamus-pituitary-adrenal axis (1st ed.).* Amsterdam: Academic. ISBN 9780444530400, (2008).

[4] JC. Pruessner, DH. Hellhammer, C. Kirschbaum, *Burnout, perceived stress, and cortisol responses to awakening.* Psychosom Med 61 (2):197-204 (1999).

[5] AJ. Douglas AJ, *Central noradrenergic mechanisms underlying acute stress responses of the Hypothalamopituitaryadrenal axis: adaptations through pregnancy and lactation.* Stress 8 (1):5-18 (2005).

[6] J. Drouin, Y. Sun, S. Tremblay, P. Lavender, T. Schmidt, A. de Lan, M. Nemer, *Homodimer formation is ratelimiting for high-affinity DNA-binding by glucocorticoid receptor.* Mol Endocrinol. 6(8):1299-1309 (1992).

[7] K. Sriram , M. Rodriguez-Fernandez, FJ. Doyle, *Modeling Cortisol Dynamics in the Neuro-endocrine Axis Distinguishes Normal, Depression, and Post-traumatic Stress Disorder (PTSD) in Humans.* PLoS Comput Biol 8(2): e1002379 (2012).

[8] GE. Miller, E. Chen, ES. Zhou, *If it goes up, must it come down? Chronic stress and the hypothalamicpituitaryadrenocortical axis in humans.* Psychological Bulletin 133 (1):25-45 (2007).

[9] R. Yehuda, *Advances in Understanding Neuroendocrine Alternations in PTSD and Their Therapeutic Implications,* Ann. N.Y. Acad.Sei. 1071 , p. 137-166 (2006).

[10] R. Yehuada, M. Teicher, R. Trestman, R. Levengood, and L. Siever , *Cortisol Regulation in Posttraumatic Stress Disorder and Major Depression: A Chronobiological Analysis,* Biol Psychiatry 40 , p. 79-88 (1996).

[11] R. Yehuda, *Post-Traumatic Stress Disorder,* N Engl J Med 2002; 346:108-114 (2002).

[12] L. Cahill, JL. McGaugh JL, *Mechanisms of emotional arousal and lasting declarative memory.* Trends Neurosci. 21 (7):294-299 (1998).

[13] N.R. Carlson, *Physiology of Behavior* , 11th Edition. New York: Allyn and Bacon. p. 605 (2010).

[14] JK. Belanoff, K. Gross, A. Yager, AF. Schatzberg, *Corticosteroids and cognition.* Journal of Psychiatric Research , Volume 35 , Issue 3 , 127-145 (2001).

[15] M. Koehl, M. Darnaudry, J. Dulluc, R.O. Van, M.M. Le, S. Maccari, *Prenatal stress alters circadian activity of hypothalamopituitaryadrenal axis and hippocampal corticosteroid receptors in adult rats of both gender.* Journal of Neurobiology 40 (3):302-315 (1999).

[16] RM. Sapolsky, *Glucocorticoids, stress and exacerbation of excitotoxic neuron death.* Seminars in Neuroscience 6 (5):323-331 (1994).

[17] SJ. Lupien, F. Maheu, M. Tu , A. Fiocco, TE. Schramek, *The effects of stress and stress hormones on human cognition: Implications for the field of brain and cognition.* Brain Cogn 65 (3):209-237 (2007).

[18] American Psychiatric Association , *Diagnostic and Statistical Manual of Mental Disorders (5th ed.).* Arlington, VA: American Psychiatric Publishing. p. 271-280 (2013).

[19] National Collaborating Centre for Mental Health (UK), *Post-Traumatic Stress Disorder: The Management of PTSD in Adults and Children in Primary and Secondary Care.*Leicester (UK): Gaskell; ISBN-10: 1-904671-25-X (2005).

[20] PR. Zoladz, DM. Diamond, *Current status on behavioral and biological markers of PTSD: A search for clarity in a conflicting literature.* Neuroscience and Biobehavioral Reviews 37(5):860-895 (2013).

[21] B. Rothschild, *The Body Remembers: The Psychophysiology of Trauma and Trauma Treatment.* New York: W.W. Norton & Company (2000).

[22] H.I. Kaplan, B.J. Sadock, J.A. Grebb, *Kaplan and Sadock's synopsis of psychiatry: Behavioral sciences, clinical psychiatry (7th ed.).* Baltimore: Williams —& Williams. p. 606-609 (1994).

[23] D. Satcher, "Chapter 4". *Mental Health: A Report of the Surgeon General.* Surgeon General of the United States (1999).

[24] R. Yehuda, S. Southwick, J. Krystal, D. Bremner, D. Charney, *Enhanced suppression of cortisol following dexamethasone administration in posttraumatic-stress-disorder.* Am J Psychiatry 150:83-86 (1993).

[25] J.R. Hughes, *Post-tetanic Potentiation.* Physiological Reviews 38 (1):91-113 (1958).

[26] K. Gerrow, A. Triller, *Synaptic stability and plasticity in a floating world.* Current Opinion in Neurobiology 20 (5):631-639 (2010).

[27] J.L. Gaiarsa, O. Caillard, Y. Ben-Ari, *Long-term plasticity at GABAergic and glycinergic synapses: mechanisms and functional significance.* Trends in Neurosciences 25 (11):564-570 (2002).

[28] SJ. Martin, PD. Grimwood, RG. Morris, *Synaptic plasticity and memory: an evaluation of the hypothesis.* Annu. Rev. Neurosci. 23:649-711 (2000).

[29] D. Purves, GJ. Augustine, D. Fitzpatrick, et al, *Neuroscience 4th ed* Sunderland,MA, Sinauer Associates,Inc. P. 177-201 (2008).

[30] EL. Bienenstock, LN. Cooper, PW. Munro, *Theory for the development of neuron selectivity: orientation specificity and binocular interaction in visual cortex.* J. Neurosci. 2 (1):32-48 (1982).

[31] CC. Bell, VZ. Han, Y. Sugawara, K. Grant, *Synaptic plasticity in a cerebellum-like structure depends on temporal order.* Nature 387:278-281 (1997).

[32] GQ. Bi, MM. Poo, *Synaptic modifications in cultured hippocampal neurons: dependence on spike timing, synaptic strength, and postsynaptic cell type.* J Neurosci 18:10464-10472 (1998).

[33] H. Markram, J. Lubke, M. Frotscher, B. Sakmann, *Regulation of synaptic efficacy by coincidence of postsynaptic APs and EPSPs.* Science 275:213-215 (1997).

[34] JC. Magee, *Dendritic hyperpolarization-activated currents modify the integrative properties of hippocampal CA1 pyramidal neurons.* J Neurosci 18:7613-7624 (1998).

[35] D.O. Hebb, *Organization of Behavior: a Neuropsychological Theory.* New York: John Wiley (1949).

[36] L.F. Abbott, S.B. Nelson, *Synaptic plasticity: taming the beast.* Nature Neuroscience 3, 1178-1183 (2000).

[37] D. Yang, MM. Poo, *Spike Timing-Dependent Plasticity: From Synapse to Perception* Physiol Rev 86: 1033-1048 (2006).

[38] F. Vinther, M. Andersen, J. Ottesen, *The minimal model of the hypothalamic-pituitary-adrenal axis,* J. Math. Biol 63, p. 663-690 (2011).

[39] S. Gupta, E. Aslakson, BM. Gurbaxani, SD. Vernon, *Inclusion of the glucocorticoid receptor in a hypothalamic pituitary adrenal axis model reveals bistability.* Theor Biol Med Model 4: 8 (2007).

[40] A. Dhooge, W. Govaerts, Yu. A. Kuznetsov, *MATCONT: A MATLAB package for numerical bifurcation analysis of ODEs.* ACM Transactions on Mathematical Software (TOMS) Volume 29 Issue 2, p. 141-164 (2003).

[41] B. Ermentrout, *Simulating, Analyzing, and Animating Dynamical Systems: A Guide Toi Xppaut for Researchers and Students* Society for Industrial and Applied Mathematics Philadelphia, PA, USA ISBN:0898715067 (2002)

[42] Yu.A. Kuznetsov, *Elements of Applied Bifurcation Theory.* Springer, 3rd edition,(2004)

[43] J. Rubin, R. Gerkin, G. Bi, and C. Chow, *Calcium Time Course as a Signal for Spike-Timing-Dependent Plasticity,* J. Neurophysiol. 93 p. 2600-2613 (2005).

[44] P. Poirazi, T. Brannon, and B.W. Mel, *Arithmetic of Subthreshold Synaptic Summation in a Model CA1 Pyramidal Cell,* Neuron, Vol. 37, 977-987, March 27, (2003).

[45] BK. Andrasfalvy, JC. Magee, *Distance-dependent increase in AMPA receptor number in the dendrites of adult hippocampal CA1 pyramidal neurons.* J Neurosci 21:9151-9159 (2001).

[46] M. Perouansky, Y. Yaari, *Kinetic properties of NMDA receptor-mediated synaptic currents in rat hippocampal pyramidal cells versus interneurones* J Physiol 465: 223-244 (1993).

BIOGRAPHICAL STATEMENT

Pengcheng Xiao was born in Xintai, Shandong Province, China. He got his Bachelor of Engineering in Information Security at China University of Mining and Technology in 2009. In August 2011, he finished his Master of Science in Mathematical Science at The University of Texas-Pan American. Starting from August 2011, Pengcheng started his doctoral study with STEM doctoral fellowship in Applied Mathematics at The University of Texas at Arlington and completed his degree in August 2015. He will start his visiting assistant professor position at University of Evansville from August 2015. In July 2013, he was selected as one of the twelve student chapters representative at Society of Industrial and Applied Mathematics Annual Conference from the whole nation. His research interests are computational neuroscience, dynamic systems, math biology modelling. He is a member of American Mathematics Society(AMS) and Society of Industrial and Applied Mathematics(SIAM) from 2011.